ACS OMEGA

Open Access

http://pubs.acs.org/journal/acsodf

Article

Application of Gelatin/Vanillin/Fe^{3+}/AGP−AgNPs Hydrogels Promotes Wound Contraction, Enhances Dermal Growth Factor Expression, and Minimizes Skin Irritation

Sarawut Lapmanee,* Sakkarin Bhubhanil, Mattaka Khongkow, Katawut Namdee, Werayut Yingmema, Narumol Bhummaphan, Prapimpun Wongchitrat, Natthawut Charoenphon, James A. Hutchison, Chanon Talodthaisong, and Sirinan Kulchat*

Cite This: *ACS Omega* 2025, 10, 10530−10545

Read Online

ACCESS | Metrics & More | Article Recommendations

ABSTRACT: This study further investigates the potential of gelatin-based hydrogel cross-linked with vanillin and ferric ion (GVF), combined with andrographolide (AGP) and silver nanoparticles (AgNPs), as an anti-infection biomaterial for wound dressing, aimed at exploring the mechanisms that attenuate inflammation, enhance wound healing rates, and address allergic skin irritation. AGP−AgNPs were evaluated for cytotoxicity in human adult epidermal keratinocytes (HEKa) and the murine macrophage cell line (RAW 264.7), as well as for nitric oxide (NO) production in response to lipopolysaccharide-induced inflammation in RAW 264.7 macrophage cells. Skin-wound specimens from male Wistar rats were histologically analyzed for epidermal thickness and inflammatory changes. The mRNA expression profiling of dermal growth factors was assessed using RT-qPCR, and skin irritation tests were conducted in female New Zealand rabbits. These AGP−AgNPs exhibited significantly lower toxicity in HEKa and no toxicity in RAW 264.7. Interestingly, AGP−AgNPs at specific concentrations produced NO in RAW 264.7 control cells but were more effective in reducing inflammatory NO levels in RAW 264.7 cells pretreated with lipopolysaccharides, suggesting that AGP−AgNP composites are safe and effectively diminish inflammation. Furthermore, a marked increase in epidermal thickness and a reduction in histological inflammatory cells at wound sites were observed in rats treated with AGP−AgNPs/GVF hydrogels over 21 days. Upregulation of dermal genes promoting wound healing, including collagen types I and III, epidermal growth factor, transforming growth factor-beta, fibronectin, and vascular endothelial growth factor, but not fibroblast growth factor, was observed in a time-dependent manner. These results suggest that the anti-inflammatory properties of GVF/AGP−AgNP hydrogels could promote epithelialization, enhance cellular proliferation, support extracellular matrix synthesis, and facilitate angiogenesis. Additionally, rabbit skin in contact with GVF/AGP−AgNP hydrogels consistently displayed reduced levels of erythema and edema, with no swelling, and a standardized scoring system yielded low primary dermal irritation indices for this hydrogel. These findings suggest that the novel GVF/AGP−AgNP hydrogels possess anti-inflammatory-like activity and can modulate dermal growth factors for wound healing. This leads to reduced dermal irritation, making the formulation potentially suitable for safe topical applications in skin and wound care. However, comprehensive human studies and clinical trials should be required in the future.

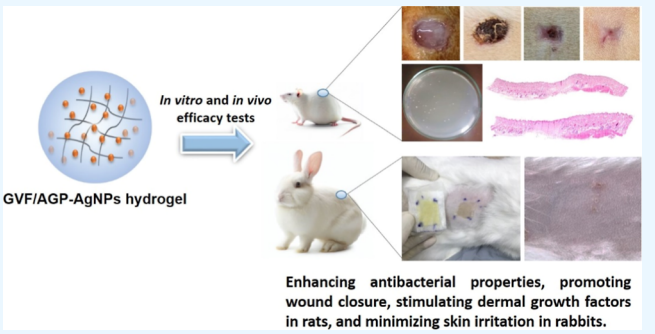

1. INTRODUCTION

Wound healing therapies and skincare have been the focus of extensive research to improve patient outcomes and minimize adverse effects. Scarring, whether resulting from injuries, surgeries, or medical conditions, can have lasting physical and psychological impacts on individuals. These effects can vary based on factors such as the size and location of the scar.[1] Scar tissue is often less flexible than surrounding skin, leading to discomfort or pain.[2]

Wound dressings play a crucial role in alleviating both the physical and psychological effects associated with myofibroblasts and keloid fibroblast formation.[3] Innovative materials like hydrogels offer significant potential benefits in this regard. Due to high water content, biocompatibility, and controlled release capabilities, hydrogels have emerged as promising

Received: December 1, 2024
Revised: February 21, 2025
Accepted: February 26, 2025
Published: March 4, 2025

carriers for bioactive compounds.[4,5] Consequently, hydrogel biomaterials have garnered considerable attention in the pharmaceutical field. Among the functional bionanomaterials, gelatin or guar gum-based hydrogels have been synthesized and employed as drug delivery systems, particularly for promoting wound healing.[6,7] Gelatin, a natural biopolymer derived from collagen, is commonly utilized in hydrogel formulations due to its biodegradability, biocompatibility, and gel-forming properties.[7,8] These gelatin-based hydrogels have shown significant potential in various biomedical applications, including wound healing, drug delivery, and tissue engineering.[9]

To enhance the properties and functionalities of hydrogels, additional components can be incorporated. One such component is vanillin, a well-known flavoring agent with antioxidant and anti-inflammatory properties.[10,11] These properties have been explored for their potential to promote wound healing, as vanillin can inhibit pro-inflammatory cytokines and enzymes, thereby reducing inflammation in experimental models.[12] Incorporating vanillin into hydrogel formulations may effectively alleviate skin irritation and improve user comfort. Interestingly, ferric metal ions, known for their involvement in numerous biological processes, have also attracted attention in cross-linked hydrogel studies.[13] These ions can interact with gelatin molecules, promoting gelation and enhancing the mechanical properties of hydrogels.[14] The inclusion of ferric ions in hydrogel formulations can improve stability and mechanical strength, thereby enhancing the performance and durability of the hydrogel as a topical formulation.[15,16] The potential applications of this hydrogel extend to the biomedical field, including wound healing and biosensors.[9,12,17]

Moreover, silver nanoparticles (AgNPs) are vital nanomaterials widely utilized in biomedical applications.[18] AgNP-embedded hydrogels play a crucial role in infection prevention and wound healing, often enhancing antibacterial activity through interactions with antibiotics or bioactive molecules by depositing on bacterial cell membranes.[6,19,20] Beyond antibiotics, the herbal antibacterial agent andrographolide (AGP), derived from *Andrographis paniculata* or *A. paniculata*, has demonstrated significant anti-inflammatory and anti-infection effects,[21] particularly on wounds and traumatic lesions. AGP also exhibits a broad spectrum of biological activities, including potent anti-inflammatory and antioxidant properties.[21−23]

Silver nanoparticle composites with andrographolide (AGP−AgNPs) have shown promising results in enhancing cell proliferation and promoting wound closure in *in vitro* scratch assays using human fibroblast cells.[24] Our study found that AGP−AgNPs integrated into hydrogels exhibit strong optical properties due to localized surface plasmon resonance and well-defined nanoscale morphology. These features enhance the biocompatibility, mechanical integrity, and potential for wound-healing applications. However, the effects of AGP−AgNPs on HEKa keratinocyte cells, which are responsible for epithelialization during dermal repair, and their potential role in regenerating the epithelial barrier remain inconclusive. To address this, ongoing studies are investigating the anti-inflammatory properties of AGP−AgNPs in the RAW 264.7 macrophage cell line exposed to lipopolysaccharide (LPS), focusing on nitric oxide (NO) production.[25]

Recently, a novel gelatin-based hydrogel cross-linked with vanillin and ferric ions (GVF) was introduced, demonstrating unique properties such as shear-thinning behavior, rapid self-healing, and high swelling capacity, making it highly suitable for wound dressing. When combined with AGP−AgNPs, GVF hydrogels exhibit exceptional physical and chemical properties, including a higher storage modulus than loss modulus, indicating a rigid and stable network. The hydrogels also demonstrate remarkable swelling capacity and a porous structure with uniformly distributed pore spaces, promoting aqueous diffusion and material homogeneity. Self-healing properties, attributed to dual cross-linking through imine and ionic bonds, enable complete recovery from mechanical disruptions.[24,26]

Additionally, GVF/AGP−AgNP hydrogels demonstrate enhanced antimicrobial properties against bacterial pathogens such as *Escherichia coli*, *Staphylococcus aureus*, and *Burkholderia pseudomallei*,[24,27] further supporting their potential in wound-healing applications. Wound healing is a complex process, where the formation of new granulation tissue and the migration of epithelial cells play pivotal roles. The healing process typically begins with coagulation and hemostasis to stop bleeding. Activated platelets within the clot release growth factors and cytokines that signal resident cells to initiate re-epithelialization, angiogenesis, and connective tissue repair.[28,29] While GVF/AGP−AgNP hydrogels have shown significant promotion of wound healing, the specific molecular mechanisms driving these effects remain unclear.

Skin irritation is another critical consideration in the formulation of topical products for cosmetics, pharmaceuticals, and personal care. To address this concern, skin irritation potential is evaluated using rabbit skin models, following the Organization for Economic Co-operation and Development (OECD) guideline number 404.[30] Skin irritation can lead to discomfort, inflammation, and undesirable reactions, undermining the effectiveness and consumer acceptance of products.[31]

This study utilized rats and rabbits, both of which are relevant models for wound healing research due to skin structure and healing processes that resemble those of humans. Rats are valuable for evaluating wound contraction rates, histopathological inflammatory changes, and underlying molecular pathways,[6,24,32] while rabbits are particularly useful for skin irritation testing due to skin similarity to that of humans.[33,34] This makes them ideal for predicting potential skin reactions and assessing erythema and edema following exposure to irritants.

As aforementioned, the aims of this study were to investigate the inflammatory effects of AGP−AgNP composites and study antimicrobial effects after application of GVF/AGP−AgNP hydrogels, as well as molecular changes impacting wound healing and evaluate skin contact safety. Additionally, we included *in vitro* inflammation tests and animal studies to examine histological changes and mRNA expression profiles of dermal growth factors involved in wound closure and tissue remodeling. Furthermore, standardized skin irritation tests were conducted to assess the hydrogels potential for irritation. We hypothesized that AGP−AgNP composites, with anti-inflammatory properties, would be effective when combined with GVF in hydrogels. It was anticipated that GVF/AGP−AgNP hydrogels would exhibit antimicrobial effects and enhance wound contraction rates by modulating dermal growth factor mRNA expression, leading to improved epithelialization and wound healing. Moreover, we expected these hydrogels to exhibit low skin irritation potential, indicating promising therapeutic potential for skin and

https://doi.org/10.1021/acsomega.4c10648
ACS Omega 2025, 10, 10530−10545

wound care. The results for the present study highlight the potential of GVF/AGP−AgNP hydrogels to enhance wound healing while minimizing skin irritation. This demonstrates potential for clinical use, particularly in wound care, as a chemical and biological innovation for medical applications in advancing therapeutic treatments for skin injuries.

2. MATERIALS AND METHODS

2.1. Materials. *2.1.1. Reagents.* The gelatin used in this study was derived from porcine skin (CAS number 9000-70-8, product number G1890) and was sourced from Sigma-Aldrich, Darmstadt, Germany. The vanillin (CAS number 121-33-5, product number W310700) was obtained from Sigma-Aldrich, Cedex, France. The ferric (III) chloride hexahydrate (97%) was purchased from Loba Chemie Pvt Ltd., Maharashtra, Mumbai, India (CAS number 10025-77-1, product number CHM.L0382000500). The silver nitrate ($AgNO_3$, 99.9%) was obtained from Poch SA, Gliwice, Poland (CAS number 7761-88-8, product number CHM.814322777.250). AGP (9 mg/capsule, drug registration number: G 292/43, product batch code: 54109) was sourced from Khaolaor Laboratories Co., Ltd. (Samutprakarn, Thailand). In brief, dried *A. paniculata* was inspected using the Ultra Performance Liquid Chromatograph (UPLC, waters corporation, Milford, MA, USA) method, ground, and finely extracted with chloroform, hexane, methanol and ethanol. The extract was then injected to measure the AGP content. For the experiments, deionized water (DI) with a specific resistivity of 18.2 MΩ·cm was obtained from a RiOsTM Type I Simplicity 185 water purification system by Merck Millipore, Darmstadt, Germany. Additionally, dimethyl sulfoxide (DMSO) was purchased from Honeywell International, Inc., Charlotte, NC, USA (CAS number 67-68-5, product number 15615740). Potassium carbonate (K_2CO_3, ≥99.0%) was purchased from Merck Millipore (CAS number 584-08-7, product number 104928).

2.1.2. Animals. In compliance with the guidelines established by the Association for Assessment and Accreditation of Laboratory Animal Care (AAALAC) International, measures were taken to minimize the number of animals used in this study, with the goal of reducing both the number of animals and the associated suffering. In line with the 3Rs principle—replace, reduce, and refine—the number of rats (3 to 5 rats per time point) was determined based on prior studies,[6,24,32,35,36] while three rabbits per test group were deemed adequate for a comprehensive assessment of dermal irritation.[33,37]

Female rodents typically show faster wound healing due to the role of 17β-estradiol in enhancing A2A adenosine receptor-mediated angiogenesis through estrogen receptors and vascular endothelial growth factor (VEGF).[38] However, male rats are often preferred in wound healing studies due to stable hormone levels and a thicker dermis. Therefore, male rats were chosen for this study.[6,24,32,39,40]

Fifteen adult male Wistar rats (BrlHan/Jcl), weighing between 190 and 210 g and aged 8 weeks, were sourced from Nomura Siam International Co., Ltd., Bangkok, Thailand (Registration number 0105556040621, category: wholesale of live animals), certified for microbiological testing (health status: superior) by the National Laboratory Animal Center, Mahidol University (NLAC-MU), Thailand, a government agency of Mahidol University (announced in the royal gazette, volume 104, section 191, on May 20, 2009). The rats were housed in groups of 2−3 per cage with enrichment toys. Drawing from previous reports,[6,24,32] the rats were randomly divided into groups based on treatment time points, which were on days 7, 14, and 21 (5 rats per time point).

Moreover, this study selected female rabbits for skin irritation studies due to increased sensitivity to irritants compared to males. Female rabbits have thinner skin, making them more suitable for detecting minor irritations, which enhances the sensitivity and reliability of skin irritation assessments.[41−43] Therefore, in the skin irritation test, a minimum of three female New Zealand rabbits (Mlac:NZW), aged 15 weeks and weighing between 2.5 and 3.0 kg, were obtained from the NLAC-MU, which conducts strict health monitoring of the animals every three months, totaling four times per year (health status: superior). The rabbits were housed individually in a separate control room, apart from the rats.

These animals were housed in a controlled laboratory environment, maintaining a 12 h light/12 h dark cycle, a temperature of 22 ± 2 °C, and a relative humidity of 52% to 54%. The animals were provided *ad libitum* access to standard rodent chow (CP Co., Ltd., Bangkok, Thailand) and sterile reverse osmosis water.

Ethical clearance for all experimental procedures was obtained from the Animal Care Committee at Thammasat University, Thailand, certified by the International Laboratory Accreditation Cooperation (protocol number: 01/2023).

2.2. Methods. *2.2.1. Synthesis of Andrographolide−Stabilized Silver Nanoparticles (AGP−AgNPs) and the Preparation of AGP−AgNPs Composite into a Hydrogel (GVF/AGP−AgNPs).* This study utilized 0.44 nM AGP−AgNPs resulting from a concentration selected based on previous findings by Talodthaisong et al. (2023)[24] which the calculation was performed using an extinction coefficient of 31.3×10^8 $M^{-1}\cdot cm^{-1}$ at 399.7 nm for citrate-stabilized silver nanoparticles with a diameter of 18 nm. The method for determining the concentration followed the approach described by Paramelle et al. (2014).[44]

To initiate the synthesis of AGP−AgNPs, an AGP solution was prepared by dissolving 20 capsules (9 mg of AGP each) in 60 mL of DI water, stirring for 1 h, and filtering the mixture. AgNPs were then synthesized by combining 3 mL of the AGP solution with 24 mL of DI water and 3 mL of 20 mM $AgNO_3$. The mixture was stirred at room temperature for 3 h, during which the solution's color changed to red-brown, indicating the formation of AgNPs. This was further confirmed using UV−vis spectroscopy. The AGP−AgNPs exhibited a characteristic UV−vis peak at 441 nm, indicative of localized surface plasmon resonance, and the morphology, observed under transmission electron microscopy (TEM), showed a narrow size distribution with a spherical or pseudospherical shape and an average diameter of 16.85 ± 5.81 nm.[24]

Subsequently, the AGP−AgNPs composite hydrogel (GVF/AGP−AgNPs) was prepared using gelatin as the base material. Gelatin powder (0.48 g) was dissolved in 8 mL of the AGP−AgNPs solution and stirred until fully dissolved. Then, 1 mL of 20 wt % vanillin in ethanol was added to the mixture. Finally, 1 mL of 0.1 M $FeCl_3\cdot 6H_2O$ was incorporated to form the GVF/AGP−AgNPs hydrogels. Characterization revealed a rigid network, shear-thinning behavior for injectability, a porous structure for fluid diffusion, and excellent self-healing properties due to dual cross-linking via imine and ionic bonds.[24,26] Then, these AGP−AgNPs or GVF/AGP−AgNPs wound

https://doi.org/10.1021/acsomega.4c10648
ACS Omega 2025, 10, 10530−10545

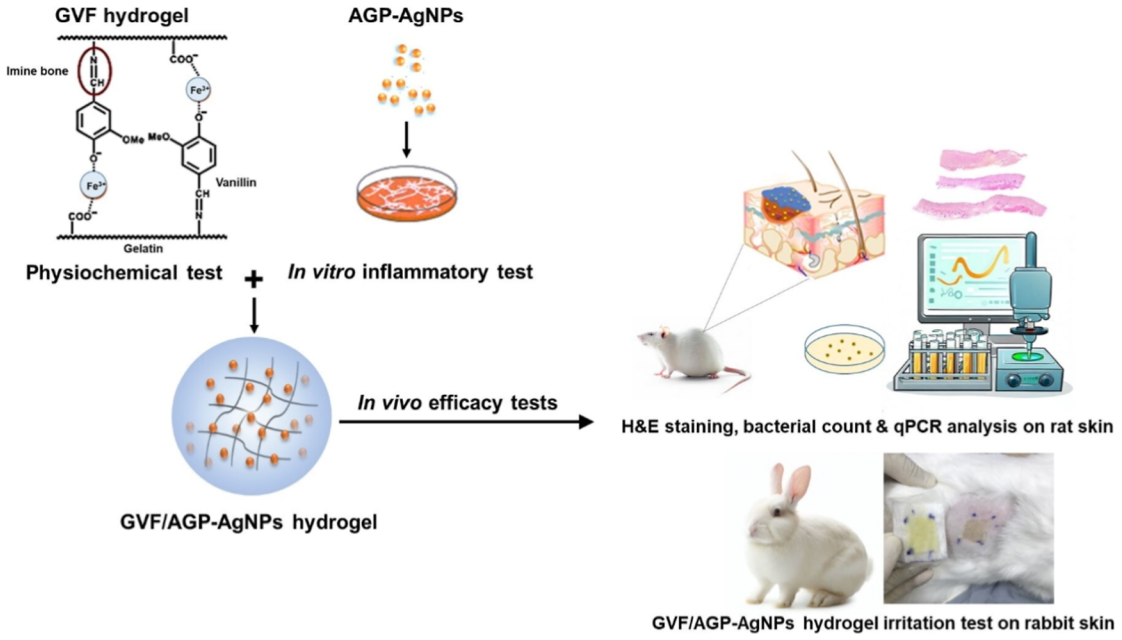

Figure 1. Experimental design in the recent study characterized GVF hydrogels incorporating AGP−AgNPs, as described by Talodthaisong et al. (2023).[24] This study examined the inflammatory response using cultured cell lines (i.e., HEKa and RAW 264.7) and evaluated GVF/AGP−AgNP hydrogels in animal models (i.e., rats and rabbits), including histological analysis, antibacterial testing, reverse transcription quantitative polymerase chain reaction (RT-qPCR) analysis in rat skin, and the rabbit skin irritation test. (Photograph courtesy of "Sarawut Lapmanee". Copyright 2024).

treatments were applied to examine efficacy in both *in vitro* and *in vivo* studies (Figure 1).

2.2.2. Assessment of Changes in Cell Viability in Cultured Cells. To evaluate the safety of AGP−AgNPs, cell viability was assessed in primary cultured cells. The human epidermal keratinocyte cell line (HEKa, ATCCPCS-200-011, USA), was selected due to its relevance in studying wound healing and inflammatory responses in the epidermis. This investigation builds upon previous work by Talodthaisong et al. (2023),[24] which focused on fibroblasts. Additionally, the mouse RAW 264.7 macrophage cell line (ATCC TIB-71, USA) was utilized to assess the effects of AGP−AgNPs before examining macrophage responses to inflammation.

Both HEKa and RAW 264.7 cells were cultured in Dulbecco's Modified Eagle's Medium (DMEM) with 10% fetal bovine serum (FBS), and incubated at 37 °C in a 5% CO_2 atmosphere. Cell viability was assessed, and 80% cell viability was considered using the 3-(4,5-dimethylthiazol-2-yl)-2,5-diphenyltetrazolium bromide (MTT) assay, following the procedures outlined by previous studies.[6,24,32] Briefly, MTT solution was added to each well and incubated for 2 h at 37 °C. The resulting blue formazan crystals were dissolved in DMSO and shaken for 10 min, and absorbance was measured at 570 nm using a microplate reader.

2.2.3. Assessment of Changes in Nitric Oxide Production in Cultured Macrophage Cells. To evaluate the inflammatory status, nitric oxide (NO) production was measured in the culture medium in response to AGP−AgNPs and anti-inflammatory activity following LPS induction. RAW 264.7 cells were incubated with gradually increasing concentrations of AGP−AgNPs for 24 h. In a separate experiment, cells were pretreated with LPS for 24 h and then incubated with AGP−AgNPs for another 24 h. Thereafter, culture medium was collected, and NO levels were measured using the Griess method. Briefly, 50 μL of the supernatant was mixed with 50 μL of Griess reagent (1% sulfanilamide and 0.1% naphthyl ethylenediamine in 5% phosphoric acid) and incubated for 10 min in the dark. A nitrite standard curve from a 0.1 M $NaNO_2$ stock solution was used, and absorbance was read at 540 nm using a microplate reader.[25,35]

2.2.4. Surgical Wound Induction and Sample Collection. Following a 7 day acclimation period, each rat underwent surgical creation of two full-thickness skin incisions, each measuring 1 cm in diameter, on the dorsal region. The first wound, located in the upper part, served as the control wound, while the second wound in the lower part was treated with GVF/AGP−AgNP hydrogels. This procedure was carried out under isoflurane anesthesia and strict sterilization protocols.[6,24,32] Veterinary or animal husbandry staff observed infections and administered tramadol injections daily for 3 days to relieve pain. Rats that experienced a 20% reduction in body weight and consumed less food and water following surgery or severe infection would have been excluded from the study; however, such occurrences were not observed in the present study. Subsequently, the resulting skin wounds on the same rat were treated with either GVF/AGP−AgNPs hydrogels or GVF gels (control).

Since GVF hydrogel had a comparable effect to the positive control commercial antibacterial gel containing mupirocin (BACTEX, Samakkhi Pharmacy Co., Ltd., Bangkok, Thailand) in preliminary study, as shown by the percentage of wound contraction and bacterial colonies from skin wound swabbing, this study aimed to further compare the efficacy of GVF hydrogel with AGP/AgNPs-GVF hydrogel.

Therefore, each rat had two wounds: one treated with GVF/AGP−AgNPs and the other with GVF gels, which served as the internal control. Daily wound cleaning with normal saline was performed once per day, and the treatment was applied around the area close to the surgical wound and directly on the wound itself. Wounds were photographed on days 0, 7, 14, and 21 postwounding. Changes in wound size relative to baseline were calculated as percentages to assess healing progress. At

https://doi.org/10.1021/acsomega.4c10648
ACS Omega 2025, 10, 10530−10545

Table 1. Primer Sequences for Candidate Dermal Growth Factors in Wound Healing[a]

gene	sense primer (5′−3′)	antisense primer (5′−3′)	T_m (°C)	accession number
β-actin *(Actb)*	CCCTGGCTCCTAGCACCAT	GATAGAGCCACCAATCCACACA	55	NM_031144.3
Collagen 1 *(Col1a1)*	CATGTTCAGCTTTGTGGACCT	GCAGCTGACTTCAGGGATGT	53	NM_053304.1
Collagen 3 *(Col3a1)*	GGGATCCAATGAGGGAGAAT	CCTTGCGTGTTTGATATT	45	NM_032085.1
EGF *(Egf)*	CTCAGGCCTCTGACTCCGAA	ATGCCGACGAGTCTGAGTTG	55	NM_012842.1
FGF-2 *(Fgf2)*	GATCCCAAGCGGCTCTACTG	TAGTTTGACGTGTGGGTCGC	56	NM_019305.2
Fibronectin *(Fn1)*	TGACCCAGACTTACGGTGGCA	GGAGTAGAAGGTCCTACCGTTGTAGTG	57	NM_001038615.2
MMP-1 *(Mmp1)*	CCGGCAGAATGTGGAAACAG	GCTGCATTTGCCTCAGCTTT	55	NM_001134530.1
TGF-β1 *(Tgfb1)*	GGGCTACCATGCCAACTTCTG	GAGGGCAAGGACCTTGCTGTA	57	NM_021578.2
VEGF *(Vegf)*	GTACCTCCACCATGCCAAGT	AATAGCTGCGCTGGTAGACG	55	NM_001287107.1

[a]EGF: epidermal growth factor; FGF-2: fibroblast growth factor-2; MMP1: Matrix Metallopeptidase 1; TGF-β1: transforming growth factor; Tm: melting temperature; VEGF: vascular endothelial growth factor.

each time point (days 7, 14, and 21 post-treatment with GVF/AGP−AgNP hydrogels), rats' skin wounds and surrounding areas were swabbed with sterile cotton soaked in phosphate-buffered saline (PBS) for bacterial colony count analysis. Additionally, rats were anesthetized with an overdose of inhaled isoflurane for sampling. Skin tissue specimens were then collected for histopathological examination and mRNA expression analysis of key genes related to inflammatory profiles, epidermal thickness, and dermal growth factors.

2.2.5. Assessment of Antibacterial Activity Using Bacterial Colony Count. To evaluate the antibacterial efficacy of GVF/AGP−AgNP hydrogels, bacterial colony counts were performed on wound swabs collected from rat skin wounds. The colony-forming units (CFUs) per wound were calculated after sampling on predetermined days (i.e., day 7, day 14, and day 21). Sterile cotton swabs were used to collect samples from the wound area, carefully rolled over the surface to ensure consistent sampling. Swabs were immediately placed into sterile tubes containing 1 mL of PBS, vortexed to release bacteria, and processed for CFU analysis following procedures described in a previous study.[6,45]

2.2.6. Assessment of Changes in Wound Size, Histological Inflammation, and Skin Thickness. Wound area percentages at each time point were carefully calculated to assess healing progress. Wound areas were presented as percentages of the baseline, calculated by comparing the size of the wound at each time point (day 7, 14, 21) to the original size of the wound (day 0) and multiplying the result by 100. Histopathological images stained with H&E, taken from formalin-fixed, paraffin-embedded tissue blocks of skin specimens (n = 5/time points) obtained in the previous study,[24] were evaluated for inflammatory responses and epidermal thickness, with a specific focus on the boundaries of the epidermal area.[32,39,40] The images, imported in JPG format, were analyzed using software to count inflammatory cells per field of view (FOV), counted in 10 fields of view per group at 400× magnification, and to determine epidermal thickness (magnification = 100×, scale bars = 100 μm) by manually drawing line segments connecting the intact stratum corneum to the dermal−epidermal junction.

2.2.7. Assessment of Changes in mRNA Expression of Genes Promoting Wound Healing. Skin from the healing wound area (0.5 × 0.5 cm in size) was collected from GVF/AGP−AgNPs hydrogels (n = 5) or untreated control (GVF gel, n = 5) rats, at each time point. Total RNA from the microdissected skin tissue was extracted using TRIzol reagent (Invitrogen Life Technologies Corp, Thermo Fisher Scientific Inc., USA) in strict accordance with the manufacturer's protocol. The RNA was treated with deoxyribonuclease I (Thermo Fisher Scientific Inc., USA) to eliminate contamination with genomic DNA. RNA concentrations were determined by NanoDrop ND-2000 spectrophotometer (Thermo Scientific Inc., USA) at a wavelength of 260 nm, and RNA samples with sufficient purity A260/A280 ratios greater than 1.8 and a minimum yield of 500 ng/μL RNA were immediately reverse transcribed to complementary DNA (cDNA). The total RNAs were further used for cDNA synthesis by using the High Capacity cDNA Reverse Transcription Kit (Applied Biosystems, Thermo Fisher Scientific Inc., USA) following the manufacturer's guidelines. The master mix was prepared by combining 10X TaqMan RT Buffer, 25X dNTP Mix, 10X Random Primers, MultiScribe Reverse Transcriptase (50 U/μL), and RNase Inhibitor (20 U/μL). Ten μL of 100 ng/μL total RNA was added to 10 μL of the master mix, and the volume was adjusted to 20 μL with RNase-Free Water. The 20 μL mixture was then loaded into each well of a PCR plate. The thermal cycler was set to the following conditions: 25 °C for 10 min, 37 °C for 120 min, 85 °C for 5 min, and hold at 4 °C. The cDNA samples were diluted and used for quantitative polymerase chain reaction (qPCR) analysis.

The mRNA expression levels of genes closely associated with wound healing include *Col1a1*, *Col3a1*, *Egf*, *Fgf2*, *Fn1*, *Mmp1*, *Tgfb1*, and *Vegf* using SYBR-based methods. To normalize differences in mRNA content between samples, the β-actin (*Actb*) gene was used as an endogenous control. The primer sets underwent thorough validation for specificity and efficiency via conventional qPCR, as detailed in previous study.[6,46] A comprehensive detail of the primers and melting temperatures employed in this study is provided in Table 1. Next, diluted cDNA and primers were combined with SsoAdvanced Universal SYBR Green Supermix (Bio-Rad Laboratories, Hercules, CA, USA) in a total reaction volume of 20 μL for PCR amplification. Each PCR reaction, including sample and nontemplate control reactions, was performed in duplicate and conducted in the CFX96 Touch Real-Time PCR Detection System (Bio-Rad Laboratories).

The thermocycling program comprised 40 cycles, followed by an additional step for generating dissociation curves.[6,47,48] Briefly, the diluted cDNA and primers were combined with SsoAdvanced Universal SYBR Green Supermix (Bio-Rad Laboratories, Hercules, CA, USA) in a final reaction volume of 20 μL. The PCR reaction of all samples was run in duplicate for 40 cycles, followed by the generation of dissociation curves to determine the specificity of the PCR reaction, which was performed on the CFX96 Touch Real-Time PCR Detection

https://doi.org/10.1021/acsomega.4c10648
ACS Omega 2025, 10, 10530−10545

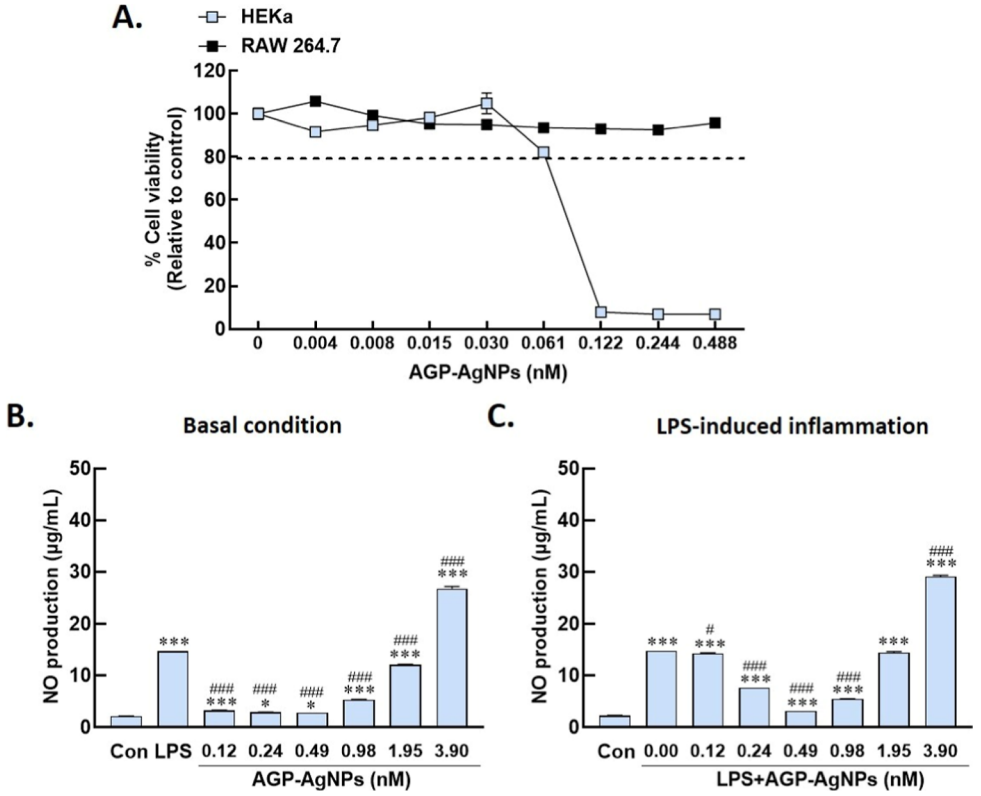

Figure 2. Effect of AGP−AgNP composites on cytotoxicity and anti-inflammation. (A) Cell viability in HEKa keratinocytes and RAW 264.7 macrophage cells, (B) nitric oxide (NO) production in RAW 264.7 control cells, and (C) pretreatment effects on LPS-induced inflammation. Data are expressed as mean ± SEM for three samples in each group. $^{*}p < 0.05$, $^{**}p < 0.01$, and $^{***}p < 0.001$ significantly different from control (untreated) and $^{\#}p < 0.05$, $^{\#\#}p < 0.01$, $^{\#\#\#}p < 0.001$ significantly different from LPS alone.

System (Bio-Rad Laboratories). No template controls were systematically included to check for contamination. In this study, the relative expression of the target genes was normalized to *Actb*. Relative mRNA expression was analyzed using CFX Manager Software (Bio-Rad Laboratories, Hercules, CA, USA) based on the comparative Ct method. The expression levels of each gene were analyzed relative to the normal levels (considered as baseline) in the untreated control group (GVF gel) of each time point and are presented as the fold change.

2.2.8. Assessment of Skin Irritation. The tests were conducted in accordance with the guidelines provided by the OECD (2015)[30] Acute dermal irritation testing of the GVF/AGP−AgNP hydrogels was performed following OECD Guideline 404 and the methods from Wang et al., (2017).[33] To prepare for the test, the fur on the dorsal area of the rabbits was shaved along the trunk (5 cm × 5 cm) approximately 24 h prior to the initiation of the experiment. For each rabbit, a 0.4 g sample of the test GVF/AGP−AgNP hydrogel was moistened with 0.5 mL of 0.9% normal saline and applied to a cotton gauze patch, securely positioned in place. A separate untreated site was designated as the control. The treated sites were observed at 3 min, 1, 4, and 24 h after application, with subsequent evaluations conducted at 48 h, 72 h, and on the seventh and 14th days thereafter. The observed reactions, including erythema, eschar formation, and edema, were assessed using a standardized scoring system for skin reactions.

Each reaction was assessed using the Draize scoring system for dermal reactions. The scores for erythema, eschar formation, and edema were summed for each time point and then divided by three to obtain the mean irritation score per time point. These mean scores were compared to those of the control sites, where sterile distilled water was applied to the animals. To determine the hazard classification based on the Primary Dermal Irritation Index (PDII), a rating scale of 0 to 5 was used, with 0 indicating no irritation and values exceeding 5.0 indicating severe irritation.[33,34,49] The PDII is calculated based on the erythema and edema scores as follows:

$$\mathrm{PDII} = \frac{S_{\mathrm{erythema,tot}} + S_{\mathrm{edema,tot}}}{N_{\mathrm{intervals}} \cdot N_{\mathrm{animals}}}$$

where $S_{\mathrm{erythema,tot}}$ and $S_{\mathrm{edema,tot}}$ are the total erythema and edema scores (all time points), respectively, $N_{\mathrm{intervals}}$ is the number of intervals, and N_{animals} is the number of animals. This standardized testing approach and scoring system allowed for the objective assessment of dermal reactions caused by the GVF/AGP−AgNP hydrogels. The PDII values obtained provide valuable information for classifying the irritant potential of these hydrogels, facilitating hazard classification and risk assessment.

2.2.9. Statistical Analysis. The data were expressed as means ± SEM. The significance of the differences between groups was analyzed by using unpaired *t*-test. The level of significance was $p < 0.05$. All statistical tests and graphs were analyzed and plotted using GraphPad Prism 10.0 (GraphPad Software Inc., San Diego, CA, USA).

3. RESULTS

3.1. Effect of AGP−AgNPs on Safety in Keratinocyte and Macrophage Cultured Cells. To evaluate the safety

https://doi.org/10.1021/acsomega.4c10648
ACS Omega 2025, 10, 10530−10545

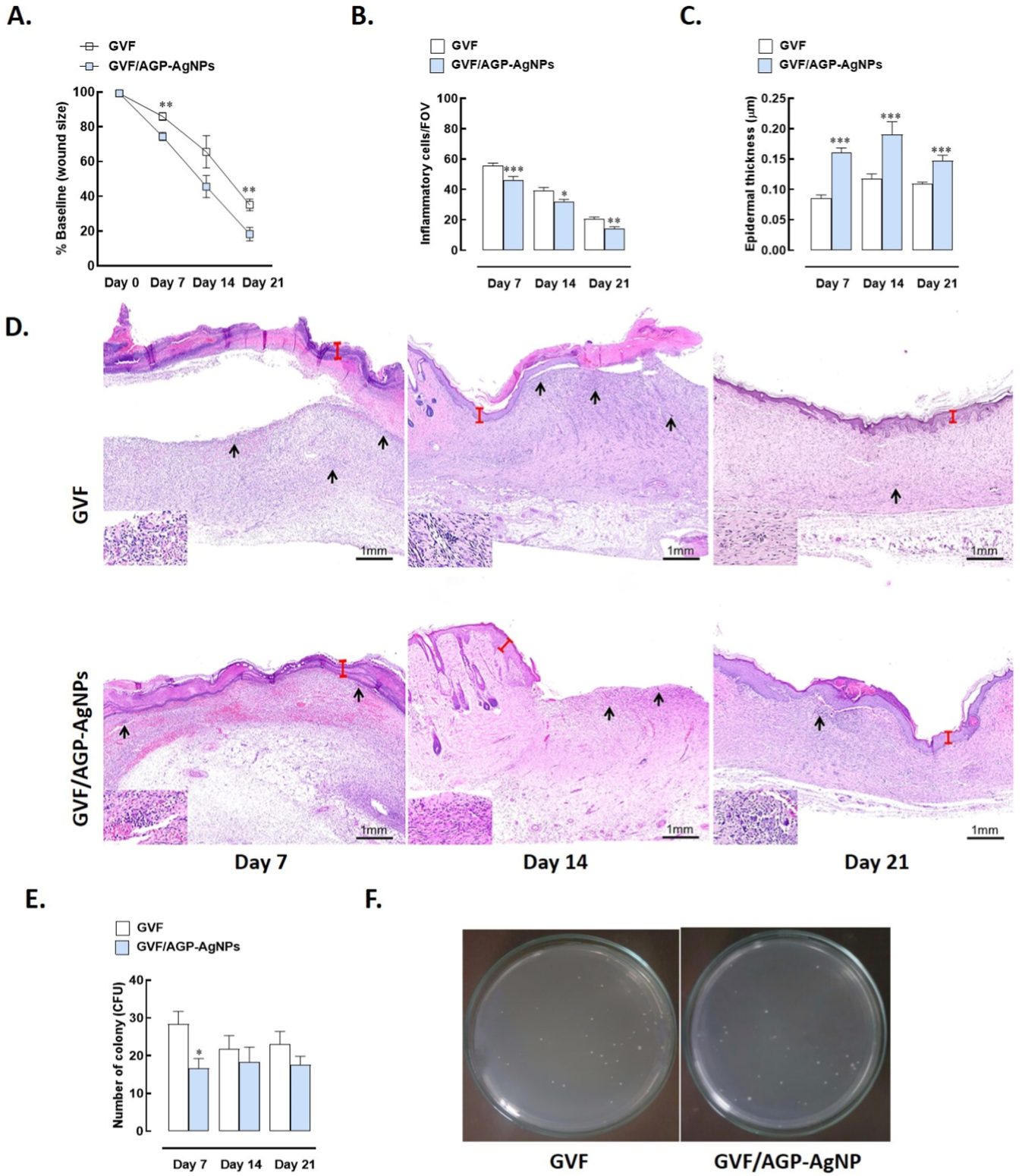

Figure 3. Effects of GVF/AGP−AgNP hydrogels on wound contraction, histological changes, and bacterial colonization. (A) Percentage change in the initial wound area over time, (B) epidermal thickness, highlighted by the red line, (C) inflammatory cells, marked by black arrows, (D) histomorphology of rat skin specimens, with a microphotograph shown in the left panel of the image, (E) number of bacterial colonies obtained from swabbing the wound site, and (F) significant bacterial presence observed on agar plates at day 7. Data are expressed as mean ± SEM for five rats in each group. Counted in 10 field of view (FOV) per group at 400× magnification. *$p < 0.05$, **$p < 0.01$, and ***$p < 0.001$ significantly different from 7 day post-treatment or control (GVF).

profile of AGP−AgNP composites, cytotoxic effects were assessed on macrophages and keratinocytes, two cell types integral to the inflammatory immune response and wound healing processes, particularly during re-epithelialization. AGP−AgNPs did not significantly impact the viability of RAW 264.7 macrophage cells, with cell viability consistently

https://doi.org/10.1021/acsomega.4c10648
ACS Omega 2025, 10, 10530−10545

remaining above 80% across all tested concentrations. Untreated control cells displayed a mean viability of 100%, indicating normal cellular function. At lower concentrations (0.004 to 0.061 nM), cell viability ranged from 105.81% to 93.65%, showing only a minor effect. Slight reductions were observed at higher concentrations (0.122 to 0.4875 nM), with viability ranging from 93.12% to 92.68%. Notably, cell viability at these higher concentrations returned to near-normal levels (95.83%) compared to the lower concentration range (Figure 2A, as indicated by the black line). These findings suggest that AGP−AgNPs do not exhibit significant cytotoxicity within the tested concentration range in RAW 264.7 macrophage cells.

Keratinocytes, the predominant cell type in the skin, are crucial for epidermal wound healing. To assess the cytotoxicity of AGP−AgNP composites, HEKa human keratinocyte cell lines were utilized. At baseline (0 nM), cell viability was 100% and remained high across concentrations from 0.004 to 0.061 nM, with viability ranging between 82.22% and 104.80%. These results indicate relative safety at these concentrations. However, a marked decline in viability was observed at 0.122 nM, with significant reductions at concentrations above 0.061 nM, indicating increased cytotoxicity (Figure 2A, as indicated by the blue line). Therefore, while AGP−AgNP composites exhibit potential therapeutic benefits, precise concentration control is crucial to minimize cytotoxic effects on keratinocytes, particularly in wound healing and skin care applications.

These results identified various AGP−AgNP concentrations that are safe for RAW 264.7 macrophage cells but become cytotoxic to HEKa human keratinocyte cell lines at concentrations exceeding 0.061 nM. This dosage is anticipated to be scaled up 10-fold (0.61 nM) for incorporation into innovative hydrogels and subsequent evaluation of wound healing efficacy in animal models. Notably, the maximum concentration of 0.44 nM AGP−AgNPs was determined based on calculations using the extinction coefficient of citrate-stabilized silver nanoparticles, as measured through UV−vis spectrophotometry.

3.2. Effect of AGP−AgNPs on Anti-Inflammation in Cultured Macrophage Cells. Since various concentrations of AGP−AgNPs did not affect the viability of RAW 264.7 macrophage cells in cytotoxicity assays, this study evaluated the ability to stimulate inflammation by generating NO, a key marker of inflammation. RAW 264.7 macrophage cells were incubated with AGP−AgNPs at concentrations starting from 0.12 nM, a level associated with keratinocyte toxicity and the potential release of NO. In the control group, baseline NO production was 2.138 μg/mL. In contrast, treatment with 1 μg/mL LPS significantly increased NO production to 14.717 μg/mL ($p < 0.001$), confirming a robust inflammatory response (Figure 2B,C).

When RAW 264.7 cells were treated with AGP−AgNPs, NO production varied significantly ($p < 0.001$). At a low concentration of 0.12 nM, NO production increased to 3.270 μg/mL. At 0.24 nM, NO levels slightly decreased to 2.893 μg/mL, and at 0.49 nM, NO levels remained stable at 2.830 μg/mL. This suggests that these lower concentrations of AGP−AgNPs may have a mild inhibitory effect on NO production. Similarly, in the LPS-treated group, a dose-dependent increase in NO production was observed with higher concentrations of AGP−AgNPs, indicating enhanced inflammation. At 0.98 nM, NO levels rose to 5.346 μg/mL, and at 1.95 nM, NO levels further increased to 12.013 μg/mL. The highest concentration tested, 3.9 nM, resulted in peak NO production of 26.792 μg/mL ($p < 0.001$). These findings suggest that higher concentrations of AGP−AgNPs could exacerbate inflammatory responses, mirroring the trend observed in the LPS-treated RAW 264.7 cells.

To evaluate the effect of anti-inflammatory AGP−AgNPs on NO production, RAW 264.7 macrophage cells pretreated with 24 h of LPS were assessed. At baseline, NO production was 2.252 μg/mL in control cells and those untreated with AGP−AgNPs. In the LPS-treated group, NO production in inflamed RAW 264.7 cells without AGP−AgNP treatment increased significantly to 14.830 μg/mL, indicating a robust inflammatory response ($p < 0.001$).

With 0.12 nM AGP−AgNPs, NO production was reduced to 14.327 μg/mL, and at 0.24 nM, it decreased further to 7.660 μg/mL, showing attenuation compared to LPS alone ($p < 0.001$). At 0.49 nM, NO production was 3.132 μg/mL, and at 0.98 nM, it was 5.459 μg/mL, suggesting a reduction in the inflammatory response ($p < 0.001$). However, markedly NO production increased to 14.453 μg/mL and 29.107 μg/mL ($p < 0.001$) at higher concentrations (1.95 and 3.9 nM, respectively), indicating a dose-dependent effect (Figure 2C). These findings suggest that AGP−AgNPs can modulate NO levels, exhibiting both inhibitory and stimulatory effects on inflammation depending on the concentration. Therefore, while AGP−AgNPs have the potential to influence inflammatory responses, careful optimization is required for therapeutic applications.

3.3. Effects of GVF/AGP−AgNP Hydrogels on Wound Contraction, Epidermal Thickness, Inflammatory Cell Recruitment, and Bacterial Colony Count in Rats. To evaluate the therapeutic effects of GVF/AGP−AgNP hydrogels, wound contraction, histological epidermal thickness, inflammatory markers, and bacterial colony counts at the wound site were assessed in rats over a 21 day period. Compared to the surgery day (day 0), the percentage of wound size relative to the initial area in the GVF/AGP−AgNPs hydrogel group significantly decreased on days 7 ($p = 0.004$) and day 21 ($p = 0.005$), with a notable trend toward significant reduction on day 14 ($p = 0.058$) as shown in the Figure 3A. Wounds in this group exhibited less inflammation, exudate, and redness, and appeared more closed and covered. This suggests that GVF/AGP−AgNPs hydrogels promote faster wound contraction and improved healing compared to the controls (GVF gels).

Histological analysis of the GVF/AGP−AgNPs hydrogel group revealed a significant increase in epidermal thickness throughout the study (Figure 3B,D), indicating enhanced wound healing compared to the control (GVF) group, which exhibited less epithelialization and thinner epidermal layers (day7, $p < 0.001$; day 14, $p = 0.006$; day 21, $p = 0.002$). The GVF/AGP−AgNPs hydrogel-treated group showed better-organized dermal structures and fewer inflammatory cells, such as neutrophils and monocytes as shown in the left panel of the photograph (Figure 3D). The number of inflammatory cells significantly decreased in the histopathological examination of the wound area at days 7, 14, and 21 post-treatment with the GVF/AGP−AgNPs hydrogel, compared to the GVF group layers (day 7, $p = 0.006$; day 14, $p = 0.011$; day 21, $p = 0.006$). This reduction in inflammatory cell infiltration suggests a more advanced stage of healing (Figure 3C,D). In addition, a significant reduction in the number of bacterial colonies on day 7 was observed in the swabbing test of wound skin treated with GVF/AGP−AgNP hydrogel compared to the GVF group ($p =$

https://doi.org/10.1021/acsomega.4c10648
ACS Omega 2025, 10, 10530−10545

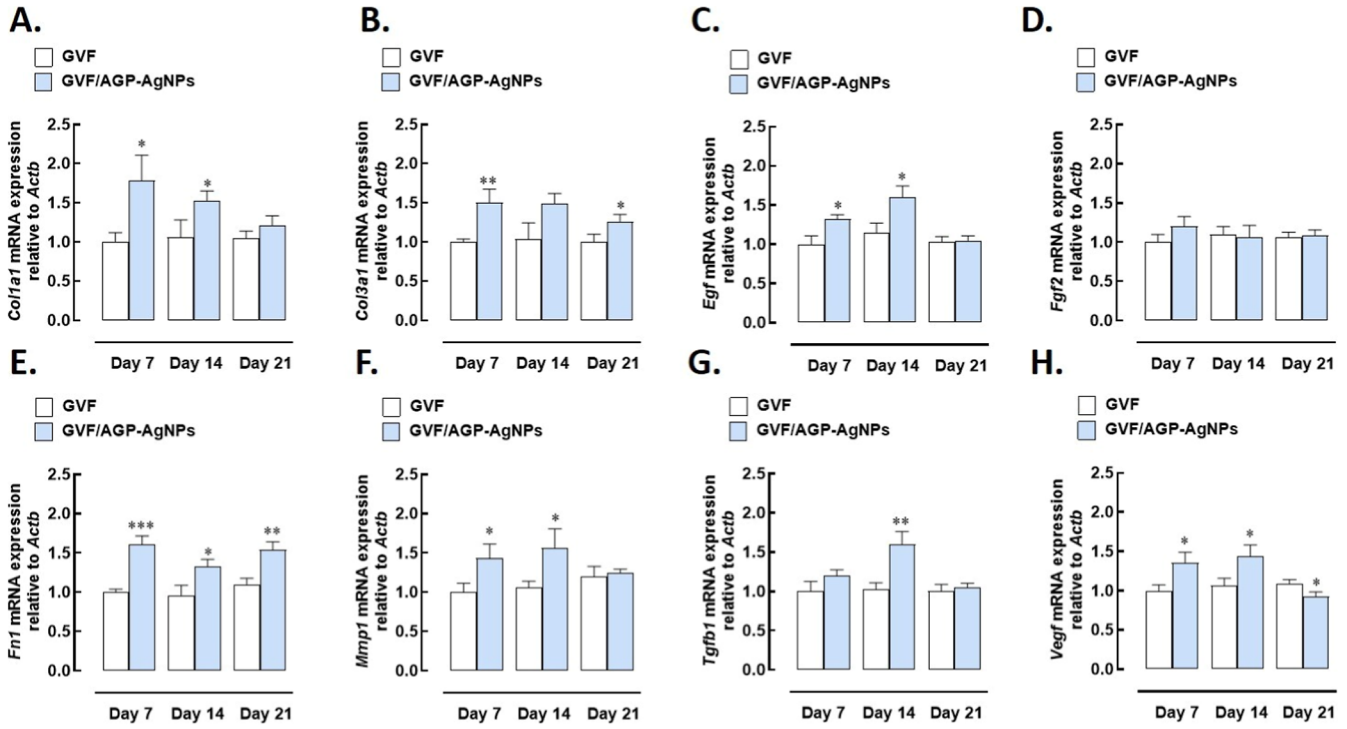

Figure 4. Effect of GVF/AGP−AgNP hydrogels on mRNA expression of dermal growth factors in wound specimen in rats. (A) Collagen type I (*Col1a1*), (B) collagen type III (*Col3a1*), (C) epidermal growth factor (*Egf*), (D) fibroblast growth factor-2 (*Fgf2*), (E) fibronectin (*Fn1*), (F) matrix metalloproteinase-1 (*Mmp1*), (G) transforming growth factor beta 1 (*Tgfb1*), and (H) vascular endothelial growth factor (*Vegf*), normalized by beta-actin in the control GVF-treated group on each day. Data are expressed as mean ± SEM for five rats in each group. *$p < 0.05$, **$p < 0.01$, and ***$p < 0.001$ significantly different from control (GVF).

0.012). These results suggest that the GVF/AGP−AgNP hydrogel exhibits antimicrobial effects.

3.4. Effect of GVF/AGP−AgNP Hydrogels on mRNA Expression of Dermal Growth Factors in Rats. To determine the therapeutic effects of GVF/AGP−AgNP hydrogels, the mRNA expression levels of key dermal growth factors, including *Col1a1*, *Col3a1*, *Egf*, *Fgf2*, *Fn1*, *Mmp1*, *Tgfb1*, and *Vegf*, were analyzed in rat skin specimens using qPCR. The GVF gel was used as the baseline control, and gene expression levels were normalized to the internal control gene, *Actb*. The GVF/AGP−AgNP hydrogels showed significant upregulation of targeted dermal growth factors on day 7 post-treatment, including *Col1a1* (78%, $p = 0.029$), *Col3a1* (51%, $p = 0.010$), *Egf* (32%, $p = 0.018$), *Fn1* (61%, $p < 0.001$), *Mmp1* (44%, $p = 0.039$), and *Vegf* (36%, $p = 0.022$). At day 14, significant upregulation continued for *Col1a1* (53%, $p = 0.05$), *Egf* (60%, $p = 0.022$), *Fn1* (33%, $p = 0.023$), *Mmp1* (57%, $p = 0.040$), *Tgfb1* (61%, $p = 0.006$), and *Vegf* (43%, $p = 0.035$). By day 21, specific upregulation persisted for *Col3a1* (27%, $p = 0.039$) and *Fn1* (54%, $p = 0.004$). However, *Vegf* mRNA expression showed a downregulation trend compared to the GVF-treated group at day 21 (−20%, $p = 0.029$), suggesting dynamic vascular remodeling and cellular responses during later stages of healing. These results highlight the potential of GVF/AGP−AgNP hydrogels to promote wound healing by enhancing epidermal growth and upregulating genes involved in skin regeneration, with time-dependent effects on vascular remodeling and tissue repair (Figure 4).

3.5. Effect of GVF/AGP−AgNP Hydrogels on Skin Irritation Test in Rabbits. To determine the safety profile of GVF/AGP−AgNP hydrogels, the study examined their effects on skin irritation in rabbits, as detailed in Table 2. Initially, skin erythema was observed at 3 min, 1 h, and 4 h after applying the hydrogel. Erythema persisted in rabbits 1 and 2 at 24 and 48 h. However, no dermal reactions were evident at 72 h or 14 days after application. The mild erythema observed at 72 h did not persist beyond 7 and 14 days (Table 2). Notably, there were no instances of edema throughout the study period (Figure 5). These findings suggest that the initial irritation was transient and resolved without long-term adverse effects. The lack of persistent irritation at 72 h and 14 days indicates that the GVF/AGP−AgNP hydrogels do not cause significant long-term skin damage or irritation. The PDII score was calculated at 0.62, indicating mild irritability according to the Draize classification. This suggests that the GVF/AGP−AgNP hydrogels caused only mild irritation, primarily reflected by the presence of skin erythema at various time points. Overall, the dermal reactions to the GVF/AGP−AgNP hydrogels were mild and transient, with no significant edema reported. These results support the biocompatibility and safety of GVF/AGP−AgNP hydrogels for potential use in wound healing applications, providing reassurance of minimal adverse effects on skin health.

4. DISCUSSION

Advancing and optimizing wound healing strategies while minimizing adverse side effects requires the application of contemporary wound closure techniques. Hydrogels, with favorable physicochemical properties, biocompatibility, and the pharmacological effects of AGP, have emerged as promising biomaterials for wound healing.[24,50]

Among natural herbal medicines, the extraction process effectively isolates the terpenoid compound AGP from *A. paniculata*. AGPs well-documented anti-inflammatory, antiox-

https://doi.org/10.1021/acsomega.4c10648
ACS Omega 2025, 10, 10530−10545

Table 2. Dermal Reactions Following Application of GVF/AGP−AgNP Hydrogels

time point	rabbit number	formation score		
		erythema & eschor	odema	total
3 min	1	1	0	1
	2	1	0	1
	3	1	0	1
1 h	1	1	0	1
	2	1	0	1
	3	1	0	1
4 h	1	1	0	1
	2	1	0	1
	3	1	0	1
24 h	1	1	0	1
	2	1	0	1
	3	0	0	0
48 h	1	1	0	1
	2	1	0	1
	3	0	0	0
72 h	1	0	0	0
	2	0	0	0
	3	0	0	0
7 days	1	0	0	0
	2	0	0	0
	3	0	0	0
14 days	1	0	0	0
	2	0	0	0
	3	0	0	0
total irritation score				13
primary irritation index ($\sum$ mean score/number of animal treated)				0.62
interpretation				slight irritation

idant, and antibacterial properties position it as a highly promising candidate for promoting and enhancing the wound healing process.[22,50−53] Furthermore, AGP exerts its antioxidant and anti-inflammatory effects by interfering with and modulating signaling pathways such as NF-κB, PI3K/Akt, MAPK, JAK/STAT, and Nrf2.[53−56] Encapsulating bioactive molecules such as curcumin, and AGP with AgNPs could enhance delivery and pharmacological action in biomedical applications.[6,24,57] This approach can play a crucial role in infection prevention and wound healing, often achieved through interaction with antibiotics, resulting in antibacterial action by deposition on the cell membrane.[6,19,20,24,58]

Our previous findings indicate that AGP incorporated with AgNPs exhibits remarkable homogeneity.[24,27] The AGP−AgNPs displayed characteristic UV−vis absorption and TEM properties, indicative of localized surface plasmon resonance. TEM showed a narrow size distribution with predominantly spherical or pseudospherical morphology, averaging a diameter of 16.85 ± 5.81 nm, making AGP−AgNPs well-suited for biomedical applications, particularly when combined with hydrogels.[24,59] Furthermore, these AGP−AgNP composites have demonstrated the ability to promote cell proliferation, effectively bridging gaps in fibroblast cells and significantly enhancing the wound healing process.[24] The present study selected HEKa keratinocytes (Figure 2A), demonstrating that these composites positively impact epithelialization during wound healing and support immune functions through antigen presentation to T-cells.[60,61] Although cell viability assays are useful for evaluating biocompatibility,[34] this study did not examine cell morphology or proliferation. However, AGP−AgNP composites showed minimal cytotoxicity in HEKa cells and maintained viability in RAW 264.7 cells (Figure 2A), indicating the safety for skin applications. A maximal dose of 0.061 nM could be scaled up by 10 to 100 times for further *in vivo* studies, remaining within a safety margin that ensures efficacy and safety.[62]

The dose−response assessment of AGP−AgNPs on HEKa cells revealed that concentrations ranging from 0 to 0.061 nM maintained over 80% cell viability, indicating biocompatibility at these levels. Conversely, exposure to 0.122 nM resulted in a significant decline in HEKa cell viability to below 15%, suggesting cytotoxic effects. However, various concentrations of AGP−AgNPs did not affect RAW 264.7 macrophages, suggesting that these cells are more resistant to AGP−AgNP exposure. Despite the cytotoxicity of 0.122 nM AGP−AgNPs on HEKa cells, this concentration exhibited potent anti-NO production activity under both basal conditions (Figure 2B) and LPS-induced inflammatory conditions (Figure 2C), suggesting its potential as an anti-inflammatory agent. These findings highlight the concentration-dependent biological activity of AGP−AgNPs. Lower concentrations support cellular viability, while higher concentrations demonstrate potential for targeted anti-inflammatory applications. This effect could be related to the suppression of NO production,[63] possibly through the inhibition of NF-κB/MAPK signaling pathways and the reduction of pro-inflammatory cytokines such as IL-1β, IL-6 and TNF-alpha in LPS-stimulated RAW264.7 cells.[64]

Our AGP−AgNPs had exhibit antibacterial activities through membrane neutralization, Ag ion release, induction of reactive oxygen species, maintenance of membrane integrity, and alteration of cell morphology.[24,27,65] Furthermore, the incorporation of bioactive compounds such as alveolar, gelatin, guar gum, and vanillin into hydrogel formulations, in combination with AgNPs, could potentially enhance the healing of skin lesions.[6,24,32,57,66] In a recent study by Talodthaisong et al. (2023),[24] GVF, consisting of gelatin, vanillin, and ferric ions, was characterized using ATR-FTIR spectra, solid-state UV−vis spectra, and exhibited a swelling degree exceeding 15,000%. When incorporated into AGP−AgNP hydrogels, GVF enhanced their mechanical and self-healing properties, as demonstrated by storage and loss moduli measurements, as well as a cut-and-self-healed sample that outperformed the uncut original piece.

Additionally, based on UV−vis absorbance measurements and the extinction coefficient of 31.3×10^8 M^{-1} cm^{-1} at 399.7 nm for 18 nm diameter citrate-coated silver nanoparticles, the appropriate concentration of AGP−AgNPs was estimated to be 0.44 nM. This concentration is less than 10 times the safety threshold (0.661 nM), which is 10 times higher than the concentration used in the cytotoxicity tests (0.061 nM). This ensures the dose remains within a safe range for future animal studies, balancing both safety and efficacy.

From a biological perspective, GVF/AGP−AgNP hydrogels promoted wound contraction in rat skin wounds. Treatment with these hydrogels resulted in a decrease in wound area relative to baseline, suggesting faster progression through the wound healing phases compared to the GVF hydrogel control group on days 7 and 21 (Figure 3A). Although a trend toward

https://doi.org/10.1021/acsomega.4c10648
ACS Omega 2025, 10, 10530−10545

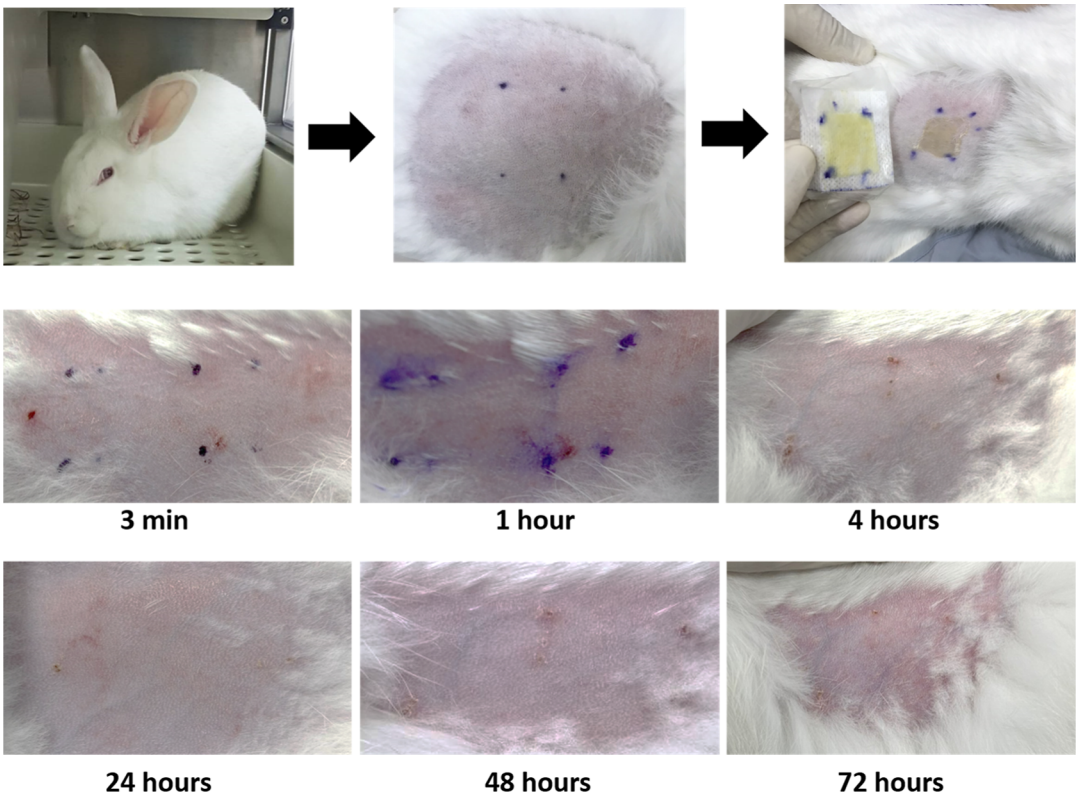

Figure 5. Study of dermal irritation in rabbits following skin contact with GVF/AGP−AgNP hydrogels. (Photograph courtesy of "Sarawut Lapmanee". Copyright 2024).

a significant reduction in wound area was observed on day 14 ($p = 0.058$), the effects of treatment are often most evident in later stages of wound healing. As reviwed by Fernández-Guarino (2023),[67] wound healing typically progresses through overlapping phases, and the benefits of GVF/AGP−AgNP hydrogels may become more pronounced during later stages, such as days 7 and 21, while earlier stages (e.g., day 14) might still be influenced by tissue remodeling or persistent inflammatory responses.

Histologically, these hydrogels markedly promoted epidermal thickness throughout the experimental period (Figure 3B). Moreover, GVF/AGP−AgNP hydrogels facilitated wound healing, particularly by reducing inflammatory cells, including mononuclear and polymorphonuclear leukocytes, in the area surrounding the wound closure. This not only suggests a decrease in inflammatory cells but also indicates a more advanced stage of tissue repair and epithelialization (Figure 3C,D). Additionally, increased collagen deposition was observed at day 14 post-treatment with GVF/AGP−AgNP hydrogels. Furthermore, the GVF/AGP−AgNP hydrogel group exhibited increased fibroblast proliferation and enhanced angiogenesis,[24] indicating improved cell interaction and tissue remodeling during the wound healing process. This suggests that GVF/AGP−AgNP hydrogels contribute to a more efficient transition through the wound dressing phases. As expected, GVF/AGP−AgNP hydrogels exhibited antimicrobial properties by reducing the number of bacteria in the swabbing test, particularly on day 7 (Figure 3E,F). These results suggest that GVF/AGP−AgNP hydrogels possess antimicrobial properties, as evidenced by the significant reduction in bacterial colony counts, particularly on day 7, indicating potential effectiveness in promoting wound healing and preventing infection.

The wound healing process generally comprises distinct phases, each involving various growth factors and cytokines.[28,29,67] It begins with the exudative inflammation phase, marked by the release of inflammatory mediators, such as procytokines, and the recruitment of immune cells in response to injury (e.g., IL-6, TNF-alpha). This is followed by the proliferation phase, characterized by granulation tissue formation, driven by growth factors such as TGF-β, FGF, and VEGF, alongside cytokines such as IL-1 and IFN-alpha. Finally, the collagen-synthesis phase culminates in scar tissue development and tissue remodeling, involving growth factors including platelet-derived growth factor, EGF, and cytokines such as IL-10, IL-35, and IFN-gamma, which are crucial for tissue repair and regeneration.[28,29,67] Since inflammation control in skin injuries significantly influences wound regeneration and repair processes, it plays a vital role in modulating dermal growth factors during wound healing.[67,68] This study, therefore, elucidated the underlying mechanisms by which AGP−AgNPs incorporated into synthetic nanohydrogels attenuate inflammation and modulate dermal growth factors.

As demonstrated by the dermal growth factor mRNA expression (Figure 4), our findings show a significant upregulation of *Col1a1*, *Col3a1*, *Egf*, *Fn1*, *Mmp1* and *Vegf* mRNA expression at day 7. This indicates that GVF/AGP−AgNP hydrogels have a rapid and positive impact on the expression of dermal growth factors critical for modifying the extracellular matrix and promoting angiogenesis in skin healing. The observed increase in collagen levels during the inflammatory phase (day 3 to 7) can be attributed to monocyte

https://doi.org/10.1021/acsomega.4c10648
ACS Omega 2025, 10, 10530−10545

induction. Neutrophils tend to induce *Tgfb1*, which promotes the conversion of fibroblasts into myofibroblasts, contributing to collagen synthesis.[28,29,69]

The sustained upregulation of *Col1a1*, *Egf*, *Fn1*, *Mmp1*, *Tgfb1*, and *Vegf* at day 14 post-GVF/AGP−AgNP hydrogel treatment indicates a lasting effect on gene expression related to matrix assembly, cell proliferation, and migration, which are crucial for tissue repair and regeneration.[28,29,67−70] Consistently, GVF/AGP−AgNP hydrogels demonstrated a significant increase in collagen content at day 14, as shown by Masson's trichrome staining. Additionally, H&E staining revealed a pro-angiogenic tendency induced by GVF/AGP−AgNP hydrogels, attributed to increased *Vegf* gene expression.[24] The upregulation of *Fn1* and *Tgfb1* genes may further support angiogenesis during the proliferation and vascular remodeling phases.[69−71]

At day 21 of GVF/AGP−AgNP hydrogels treatment, during the early remodeling stage, the continued upregulation of *Col3a1* and *Fn1* genes further supports their enduring impact on extracellular matrix remodeling, re-epithelialization, and nearly completed vascular remodeling. This is indicated by the downregulation of *Vegf* expression, along with observable wound contraction and scar formation.[72]

In addition, although *Fgf2* mRNA expression remained unchanged (Figure 4D) in GVF/AGP−AgNP hydrogels treatment, it functionally binds to specific dermal fibroblasts and contributes to extracellular vesicle formation, preventing degradation and supporting cell migration, differentiation, and vascular angiogenesis.[73] Therefore, the intricate coordination of dermal growth factors by GVF/AGP−AgNP hydrogels, including *Col1a1*, *Col3a1*, *Egf*, *Fn1*, *Mmp1*, *Tgfb1*, and *Vegf*, ensures efficient wound healing by facilitating the transition from homeostasis and inflammation to tissue proliferation and remodeling.[70,74,75] These results underscore the importance of evaluating GVF/AGP−AgNP hydrogels in understanding the wound healing process. Nevertheless, the study also assessed the risk of adverse skin reactions.

The results from the skin irritation study indicate the safety and potential for sensitization of GVF/AGP−AgNP hydrogels when applied to the skin. At the earliest time points (3 min to 4 h postapplication), all rabbits exhibited erythema and eschar with scores of 1, suggesting an immediate, mild irritation. This initial irritation reflects a transient activation of the innate immune system in response to direct skin contact, rather than an allergic reaction.[76] The assessment of skin irritation also included evaluating redness due to capillary hyperemia and observing fluid swelling in the test skin tissue.[33,34,39] It is important to note that the skin irritation scoring system, which assesses erythema and edema in rabbit skin, may be influenced by factors such as thicker and more pigmented skin associated with hair growth, potentially affecting the accuracy of the results.[34] This study revealed that GVF/AGP−AgNP hydrogels caused dermal reactions and irritability on rabbit skin, particularly during the initial period after hydrogel removal.

Over time, irritation scores showed a marked reduction. By 24 h, irritation had decreased from the initial symptoms. By 48 h, most rabbits showed no signs of irritation. At 72 h and 14 days, there were no signs of erythema, eschar, or edema, demonstrating that the irritation caused by the GVF/AGP−AgNP hydrogels was transient and resolved within a few days. These results confirm that the irritation was temporary and resolved promptly (Figure 5), suggesting that the GVF/AGP−AgNP hydrogels did not induce persistent or long-term skin irritation. Therefore, AGP−AgNPs demonstrated a potential inflammatory response to dermal contact with synthetic GVF hydrogels, resembling the response observed in a *S. aureus*-induced rabbit dermatitis, which may have mitigated irritant effects.[77,78]

However, this study has several limitations. It did not examine the hydrogel's degradation rate over time or the release kinetics of AGP−AgNPs from the hydrogel. Additionally, the small animal sample size suggests that further research with a larger sample is needed to validate these findings. Furthermore, a broader range of dermal growth factors, cytokine profiles, and specific protein expressions were not assessed through methods such as immunohistochemistry and Western blotting. Aspects such as wound strength and scar formation were also not assessed, and these should be explored in future studies. While this study demonstrates that GVF/AGP−AgNP hydrogels are safe with minimal irritation in the rabbit skin irritation test, future mechanistic studies should focus on the rabbit model. This includes histological analysis of the epidermal and dermal layers, evaluation of signs of inflammation (e.g., hyperemia, edema, and cell infiltration), and identification of potential tissue damage or healing effects. Additionally, the distribution and localization of AGP−AgNPs in skin tissues should be evaluated using fluorescent labeling or electron microscopy. This will help determine if nanoparticles accumulate in the skin and how they might impact the skin barrier function or induce local irritation. Further, the potential immune response triggered by the GVF/AGP−AgNP hydrogels should be assessed by measuring the expression of pro-inflammatory cytokines in the skin after hydrogel application. This could help determine whether the hydrogels induce any systemic or local immune responses, leading to skin irritation. Finally, a skin sensitivity test in human studies would be necessary to evaluate dermal responses following the application of GVF/AGP−AgNP hydrogels.

In summary, this study explores the potential of anti-inflammatory GVF hydrogels incorporating AGP−AgNPs to enhance wound healing rates, promote complete epidermal thickness, regulate dermal growth factors, and mitigate skin irritation. While previous study by Talodthaisong et al. (2023)[24] has demonstrated significant promise for GVF/AGP−AgNP hydrogels in wound healing, gaps remain in understanding the precise inflammation modulation and molecular mechanisms driving this process, as well as their impact on skin irritation. The AGP−AgNP composites exhibited low toxicity in keratinocytes and macrophage-cultured cells and also demonstrated anti-inflammatory effects by reducing NO production within a safe concentration range. Following treatment with GVF/AGP−AgNP hydrogels, the healing process accelerated with epidermal growth, possibly due to the modulation of inflammatory cell recruitment, as determined by histological analysis. At the 7 day mark, significant upregulation of mRNA for dermal growth factor genes, including *Col1a1*, *Col3a1*, *Egf*, *Fn1*, *Mmp1*, and *Vegf*, was observed, indicating enhanced wound closure and tissue remodeling. Subsequently, on days 14 and 21, there was continued upregulation of *Col1a1*, *Col3a1*, *Egf*, *Fn1*, *Mmp1*, *Tgfb1*, and *Vegf* These findings suggested enhanced cellular proliferation, extracellular matrix synthesis, and angiogenesis, further promoting continuous wound healing and tissue regeneration. Throughout the observation period, the areas treated with GVF/AGP−AgNP hydrogels consistently displayed reduced levels of erythema and edema compared to control sites. Furthermore, the implementation of a stand-

https://doi.org/10.1021/acsomega.4c10648
ACS Omega 2025, 10, 10530−10545

ardized scoring system resulted in low primary dermal irritation indices for GVF/AGP−AgNP hydrogels. Collectively, these findings support the feasibility of developing safer topical formulations for wound care. The promising results obtained warrant further exploration, including human studies and clinical trials, to advance wound healing therapies and skincare.

■ ASSOCIATED CONTENT

Data Availability Statement

All data in this study are present in the manuscript.

■ AUTHOR INFORMATION

Corresponding Authors

Sarawut Lapmanee − *Chulabhorn International College of Medicine, Thammasat University, Pathumthani 10120, Thailand; Department of Basic Medical Sciences, Faculty of Medicine, Siam University, Bangkok 10160, Thailand;* orcid.org/0000-0002-8890-9109; Phone: +66-2-564 4440; Email: lapmanee@tu.ac.th

Sirinan Kulchat − *Department of Chemistry and Center of Excellence for Innovation in Chemistry, Faculty of Science, Khon Kaen University, Khon Kaen 40002, Thailand;* orcid.org/0000-0002-2411-7495; Phone: +66-430-09700 ext. 42174; Email: sirikul@kku.ac.th; Fax: +66-432-02373

Authors

Sakkarin Bhubhanil − *Department of Basic Medical Sciences, Faculty of Medicine, Siam University, Bangkok 10160, Thailand*

Mattaka Khongkow − *National Science and Technology Development Agency, National Nanotechnology Centre, Pathumthani 12120, Thailand;* orcid.org/0000-0002-4424-8898

Katawut Namdee − *National Science and Technology Development Agency, National Nanotechnology Centre, Pathumthani 12120, Thailand;* orcid.org/0000-0003-3763-9388

Werayut Yingmema − *Laboratory Animal Center, Thammasat University, Pathumthani 10120, Thailand*

Narumol Bhummaphan − *College of Public Health Sciences, Chulalongkorn University, Bangkok 10330, Thailand*

Prapimpun Wongchitrat − *Center for Research Innovation and Biomedical Informatics, Faculty of Medical Technology, Mahidol University, Nakhon Pathom 73170, Thailand*

Natthawut Charoenphon − *Department of Anatomy, Faculty of Medical Science, Naresuan University, Phitsanulok 65000, Thailand*

James A. Hutchison − *School of Chemistry and Centre of Excellence in Exciton Science, The University of Melbourne, Parkville, Victoria 3010, Australia;* orcid.org/0000-0002-0595-9961

Chanon Talodthaisong − *Department of Chemistry and Center of Excellence for Innovation in Chemistry, Faculty of Science, Khon Kaen University, Khon Kaen 40002, Thailand*

Complete contact information is available at: https://pubs.acs.org/10.1021/acsomega.4c10648

Author Contributions

S.L. and S.K.; methodology, S.L., S.B. and C.T.; validation, S.L., S.B., C.T., W.Y., and P.W.; formal analysis, S.L., W.Y., N.B.; investigation, S.L., S.B., C.T., N.B., P.W., W.Y., M.K., and K.N.; resources, S.L. and S.K.; data curation, S.L., S.B., C.T., N.B., P.W., W.Y., M.K., and K.N.; writing—original draft preparation, S.L., S.K., P.W., and J.A.H.; writing—review and editing, S.L., S.K., JAH.; visualization, S.L., C.T., S.K., and JAH; supervision, S.L. and S.K.; project administration, S.L. and S.K.; funding acquisition, S.L., S.K, M.K., and K.N. All authors read and approved the final version of the manuscript.

Funding

This work was supported by research grant support received from the Fundamental Fund 2566 of Thailand Science Research and Innovation through Siam University (grant number 01/2566 to S.L.). Additional thanks go to the Research Top-up Grant for the Academic Year 2023 from the Faculty of Medicine, Siam University (MEDSIAM 01/2566) to S.L. Financial support received from The Science Achievement Scholarship of Thailand (SAST) and Faculty of Science, Khon Kaen University to C.T (KKU 01/2559). S.K. thanks The Outbound Visiting Scholar program, Khon Kaen University, which provided both financial assistance and access to laboratory resources (academic year 2021). Furthermore, we express our gratitude to the National Science and Technology Development Agency (NSTDA, Thailand) for the Target Development Group grant (Cosmeceuticals) P1952244 awarded to M.K. and K.N. In addition, J. A. H. received funding from the Australian Research Council (ARC) Future Fellowship (FT180100295) and the Centre of Excellence in Exciton Science (CE170100026).

Notes

The authors declare no competing financial interest.

■ ACKNOWLEDGMENTS

We would like to thank Apichart Saenchoopa from the Materials Chemistry Research Center, Department of Chemistry, Center of Excellence for Innovation in Chemistry, Faculty of Science, Khon Kaen University, and Phichaporn Bunwatcharaphansakun from the National Nanotechnology Centre, National Science and Technology Development Agency, for their excellent assistance. We also appreciate Siriwan Sriwong from the Laboratory Animal Center, Thammasat University, for her excellent animal handling and for collecting specimens.

■ REFERENCES

(1) Ziolkowski, N.; Kitto, S. C.; Jeong, D.; Zuccaro, J.; Adams-Webber, T.; Miroshnychenko, A.; Fish, J. S. Psychosocial and quality of life impact of scars in the surgical, traumatic and burn populations: a scoping review protocol. *BMJ Open* **2019**, *9*, No. e021289.

(2) Abd-Elsayed, A.; Pope, J.; Mundey, D. A.; Slavin, K. V.; Falowski, S.; Chitneni, A.; Popielarski, S. R.; John, J.; Grodofsky, S.; Vanetesse, T.; Fishman, M. A.; Kim, P. Diagnosis, treatment, and management of painful scar: a narrative review. *J. Pain Res.* **2022**, *15*, 925−937.

(3) Zhang, L.; Tai, Y.; Liu, X.; Liu, Y.; Dong, Y.; Liu, Y.; Yang, C.; Kong, D.; Qi, C.; Wang, S.; Midgley, A. C. Natural polymeric and peptide-loaded composite wound dressings for scar prevention. *Appl. Mater. Today* **2021**, *25*, 101186.

(4) Hu, W.; Yang, C.; Guo, X.; Wu, Y.; Loh, X. J.; Li, Z.; Wu, Y. L.; Wu, C. Research advances of injectable functional hydrogel materials in the treatment of myocardial infarction. *Gels* **2022**, *8*, 423.

(5) Thang, N. H.; Chien, T. B.; Cuong, D. X. Polymer-based hydrogels applied in drug delivery: an overview. *Gels* **2023**, *9*, 523.

(6) Bhubhanil, S.; Talodthaisong, C.; Khongkow, M.; Namdee, K.; Wongchitrat, P.; Yingmema, W.; Hutchison, J. A.; Lapmanee, S.; Kulchat, S. Enhanced wound healing properties of guar gum/curcumin-stabilized silver nanoparticle hydrogels. *Sci. Rep.* **2021**, *11*, 21836.

(7) Andreazza, R.; Morales, A.; Pieniz, S.; Labidi, J. Gelatin-based hydrogels: potential biomaterials for remediation. *Polymers* **2023**, *15*, 1026.
(8) Piao, Y.; You, H.; Xu, T.; Bei, H. P.; Piwko, I. Z.; Kwan, Y. Y.; Zhao, X. Biomedical applications of gelatin methacryloyl hydrogels. *Eng. Regener.* **2021**, *2*, 47−56.
(9) Cao, H.; Wang, J.; Hao, Z.; Zhao, D. Gelatin-based biomaterials and gelatin as an additive for chronic wound repair. *Front. Pharmacol.* **2024**, *15*, 1398939.
(10) Xiong, S.; Li, R.; Ye, S.; Ni, P.; Shan, J.; Yuan, T.; Liang, J.; Fan, Y.; Zhang, X. Vanillin enhances the antibacterial and antioxidant properties of polyvinyl alcohol-chitosan hydrogel dressings. *Int. J. Biol. Macromol.* **2022**, *220*, 109−116.
(11) Zhu, Z.; Yu, Q.; Li, H.; Han, F.; Guo, Q.; Sun, H.; Zhao, H.; Tu, Z.; Liu, Z.; Zhu, C.; Li, B. Vanillin-based functionalization strategy to construct multifunctional microspheres for treating inflammation and regenerating intervertebral disc. *Bioact. Mater.* **2023**, *28* (28), 167−182.
(12) Costantini, E.; Sinjari, B.; Falasca, K.; Reale, M.; Caputi, S.; Jagarlapodii, S.; Murmura, G. Assessment of the vanillin anti-inflammatory and regenerative potentials in inflamed primary human gingival fibroblast. *Mediators Inflammation* **2021**, *2021*, 5562340.
(13) Ge, S.; Ji, N.; Cui, S.; Xie, W.; Li, M.; Li, Y.; Xiong, L.; Sun, Q. Coordination of covalent cross-linked gelatin hydrogels via oxidized tannic acid and ferric ions with strong mechanical properties. *J. Agric. Food Chem.* **2019**, *67*, 11489−11497.
(14) Anamizu, M.; Tabata, Y. Design of injectable hydrogels of gelatin and alginate with ferric ions for cell transplantation. *Acta Biomater.* **2019**, *100*, 184−190.
(15) Huang, Y.; Liu, J.; Wang, J.; Hu, M.; Mo, F.; Liang, G.; Zhi, C. An intrinsically self-healing NiColl Zn rechargeable battery with a self-healable ferric-ion-crosslinking sodium polyacrylate hydrogel electrolyte. *Angew. Chem., Int. Ed.* **2018**, *57*, 9810−9813.
(16) Shams, F.; Moravvej, H.; Hosseinzadeh, S.; Mostafavi, E.; Bayat, H.; Kazemi, B.; Bandehpour, M.; Rostami, E.; Rahimpour, A.; Moosavian, H. Overexpression of VEGF in dermal fibroblast cells accelerates the angiogenesis and wound healing function: in vitro and in vivo studies. *Sci. Rep.* **2022**, *12*, 18529.
(17) Kim, N. G.; Chandika, P.; Kim, S. C.; Won, D. H.; Park, W. S.; Choi, I. W.; Lee, S. G.; Kim, Y. M.; Jung, W. K. Fabrication and characterization of ferric ion cross-linked hyaluronic acid/pectin-based injectable hydrogel with antibacterial ability. *Polymer* **2023**, *271*, 125808.
(18) Babu, P. J.; Tirkey, A.; Paul, A. A.; Kristollari, K.; Barman, J.; Panda, K.; Sinha, N.; Babu, B. R.; Marks, R. S. Advances in nano silver-based biomaterials and their biomedical applications. *Eng. Regener.* **2024**, *5*, 326−341.
(19) Qing, Y.; Cheng, L.; Li, R.; Liu, G.; Zhang, Y.; Tang, X.; Wang, J.; Liu, H.; Qin, Y. Potential antibacterial mechanism of silver nanoparticles and the optimization of orthopedic implants by advanced modification technologies. *Int. J. Mol. Sci.* **2018**, *13*, 3311−3327.
(20) Saenchoopa, A.; Boonta, W.; Talodthaisong, C.; Srichaiyapol, O.; Patramanon, R.; Kulchat, S. Colorimetric detection of Hg(II) by γ-aminobutyric acid-silver nanoparticles in water and the assessment of antibacterial activities. *Spectrochim. Acta, Part A* **2021**, *251*, 119433.
(21) Li, R.; Liu, K.; Huang, X.; Li, D.; Ding, J.; Liu, B.; Chen, X. Bioactive materials promote wound healing through modulation of cell Behaviors. *Adv. Sci.* **2022**, *9*, No. e2105152.
(22) Mussard, E.; Cesaro, A.; Lespessailles, E.; Legrain, B.; Berteina-Raboin, S.; Toumi, H. Andrographolide, a natural antioxidant: an update. *Antioxidants* **2019**, *8*, 571.
(23) Li, X.; Yuan, W.; Wu, J.; Zhen, J.; Sun, Q.; Yu, M. Andrographolide a natural anti-inflammatory agent: an update. *Front. Pharmacol* **2022**, *13*, 920435.
(24) Talodthaisong, C.; Patramanon, R.; Thammawithan, S.; Lapmanee, S.; Maikaeo, L.; Sricharoen, P.; Khongkow, M.; Namdee, K.; Jantimaporn, A.; Kayunkid, N.; Hutchison, J. A.; Kulchat, S. A shear-thinning, self-healing, dual-cross linked hydrogel based on gelatin/vanillin/Fe^{3+}/AGP-AgNPs: synthesis, antibacterial, and wound-healing assessment. *Macromol. Biosci.* **2023**, *23*, No. e2300250.
(25) Cao, Y.; Chen, J.; Ren, G.; Zhang, Y.; Tan, X.; Yang, L. Punicalagin prevents inflammation in LPS-induced RAW264.7 macrophages by inhibiting FoxO3a/autophagy signaling pathway. *Nutrients* **2019**, *11*, 2794.
(26) Han, N.; Xu, Z.; Cui, C.; Li, Y.; Zhang, D.; Xiao, M.; Fan, C.; Wu, T.; Yang, J.; Liu, W. A Fe^{3+}-crosslinked pyrogallol-tethered gelatin adhesive hydrogel with antibacterial activity for wound healing. *Biomater. Sci.* **2020**, *8* (11), 3164−3172.
(27) Thammawithan, S.; Talodthaisong, C.; Srichaiyapol, O.; Patramanon, R.; Hutchison, J. A.; Kulchat, S. Andrographolide stabilized-silver nanoparticles overcome ceftazidime-resistant *Burkholderia pseudomallei*: study of antimicrobial activity and mode of action. *Sci. Rep.* **2022**, *12*, 10701.
(28) Peña, O. A.; Martin, P. Cellular and molecular mechanisms of skin wound healing. *Nat. Rev. Mol. Cell Biol.* **2024**, *25*, 599−616.
(29) Farhangniya, M.; Samadikuchaksaraei, A. A review of genes involved in wound healing. *Med. J. Islam. Repub. Iran.* **2023**, *37*, 140.
(30) OECD *Acute dermal irritation/corrosion OECD guidelines for the testing of chemicals*; OECD: Paris, France, 2015; .
(31) Kaushik, M.; Farooq, U.; Ali, M. S.; Ansari, M. J.; Iqbal, Z.; Mirza, M. A. Safety concern and regulatory status of chemicals used in cosmetics and personal care products. *Dermato* **2023**, *3*, 131−157.
(32) Lapmanee, S.; Bhubhanil, S.; Charoenphon, N.; Inchan, A.; Bunwatcharaphansakun, P.; Khongkow, M.; Namdee, K. Cannabidiol-loaded lipid nanoparticles incorporated in polyvinyl alcohol and sodium alginate hydrogel scaffold for enhancing cell migration and accelerating wound healing. *Gels* **2024**, *10* (12), 843.
(33) Wang, J.; Li, Z.; Sun, F.; Tang, S.; Zhang, S.; Lv, P.; Li, J.; Cao, X. Evaluation of dermal irritation and skin sensitization due to vitacoxib. *Toxicol Rep* **2017**, *4*, 4287−4290.
(34) Rooney, J. P.; Choksi, N. Y.; Ceger, P.; Daniel, A. B.; Truax, J.; Allen, D.; Kleinstreuer, N. Analysis of variability in the rabbit skin irritation assay. *Regul. Toxicol. Pharmacol.* **2021**, *122*, 104920.
(35) Guerrero-Juarez, C. F.; Astrowski, A. A.; Murad, R.; Dang, C. T.; Shatrova, V. O.; Astrowskaja, A.; Lim, C. H.; Ramos, R.; Wang, X.; Liu, Y.; Lee, H. L.; Pham, K. T.; Hsi, T. C.; Oh, J. W.; Crocker, D.; Mortazavi, A.; Ito, M.; Plikus, M. V. Wound regeneration deficit in rats correlates with low morphogenetic potential and distinct transcriptome profile of epidermis. *J. Invest. Dermatol.* **2018**, *138*, 1409−1419.
(36) Hamada, T.; Matsubara, H.; Yoshida, Y.; Ugaji, S.; Nomura, I.; Tsuchiya, H. Autologous adipose-derived stem cell transplantation enhances healing of wound with exposed bone in a rat model. *PLoS One* **2019**, *14*, No. e0214106.
(37) Kongkon, P.; Pichayakorn, W.; Sanohkan, S. Evaluation of in vivo bond strength and skin irritation test for new skin adhesive. *J. Oral. Biol. Craniofac. Res.* **2023**, *13*, 731−738.
(38) Troncoso, F.; Herlitz, K.; Acurio, J.; Aguayo, C.; Guevara, K.; Castro, F. O.; Godoy, A. S.; San Martin, S.; Escudero, C. Advantages in wound healing process in female mice require upregulation A2A-mediated angiogenesis under the stimulation of 17β-estradiol. *Int. J. Mol. Sci.* **2020**, *21*, 7145.
(39) Masson-Meyers, D. S.; Andrade, T. A. M.; Caetano, G. F.; Guimaraes, F. R.; Leite, M. N.; Leite, S. N.; Frade, M. A. C. Experimental models and methods for cutaneous wound healing assessment. *Int. J. Exp. Pathol.* **2020**, *101*, 21−37.
(40) Salari Rafsanjani, M.; Tabatabaei Naeini, A.; Meimandi-Parizi, A.; Nowzari, F.; Mujtaba Wani, M.; Iraji, A.; Iraji, A. Wound healing effect of *Carum carvi L.* on the incised skin wound in male rats: histopathology, total protein and biomechanical evaluations. *Vet. Med. Sci.* **2022**, *8*, 2726−2737.
(41) Lulekal, E.; Tesfaye, S.; Gebrechristos, S.; Dires, K.; Zenebe, T.; Zegeye, N.; Feleke, G.; Kassahun, A.; Shiferaw, Y.; Mekonnen, A. Phytochemical analysis and evaluation of skin irritation, acute and

https://doi.org/10.1021/acsomega.4c10648
ACS Omega 2025, 10, 10530−10545

sub-acute toxicity of Cymbopogon citratus essential oil in mice and rabbits. *Toxicol Rep* **2019**, *6*, 1289−1294.
(42) LeFors, J. E.; Anderson, L. M.; Hanson, M. A.; Raiciulescu, S. Assessment of 2 hair removal methods in New Zealand white rabbits (Oryctolagus cuniculus). *J. Am. Assoc. Lab. Anim. Sci.* **2022**, *61*, 296−303.
(43) Moroki, T. Morphological characteristics and notes of the skin in preclinical toxicity assessment. *J. Toxicol. Pathol.* **2023**, *36*, 85−94.
(44) Paramelle, D.; Sadovoy, A.; Gorelik, S.; Free, P.; Hobley, J.; Fernig, D. G. A rapid method to estimate the concentration of citrate capped silver nanoparticles from UV-visible light spectra. *Analyst* **2014**, *139* (19), 4855−4861.
(45) Kumarajith, T. M.; Powell, S. M.; Breadmore, M. C. Isotachophoretic quantification of total viable bacteria on meat and surfaces. *Anal. Chim. Acta* **2024**, *1296*, 342253.
(46) Gushiken, L. F. S.; Hussni, C. A.; Bastos, J. K.; Rozza, A. L.; Beserra, F. P.; Vieira, A. J.; Padovani, C. R.; Lemos, M.; Polizello Junior, M.; Silva, J. J. M. d.; Nóbrega, R. H.; Martinez, E. R. M.; Pellizzon, C. H. Skin wound healing potential and mechanisms of the hydroalcoholic extract of leaves and oleoresin of copaifera langsdorffii desf. kuntze in rats. *Evidence-Based Complementary Altern. Med.* **2017**, *2017*, 6589270.
(47) Wongchitrat, P.; Pakpian, N.; Kitidee, K.; Phopin, K.; Dharmasaroja, P. A.; Govitrapong, P. Alterations in the expression of amyloid precursor protein cleaving enzymes mRNA in Alzheimer peripheral blood. *Curr. Alzheimer Res.* **2018**, *16*, 29−38.
(48) Pakpian, N.; Phopin, K.; Kitidee, K.; Govitrapong, P.; Wongchitrat, P. Alterations in mitochondrial dynamic-related genes in the peripheral blood of Alzheimer's disease patients. *Curr. Alzheimer Res.* **2020**, *17* (7), 616−625.
(49) Charmeau-Genevois, C.; Sarang, S.; Perea, M.; Eadsforth, C.; Austin, T.; Thomas, P. A simplified index to quantify the irritation/corrosion potential of chemicals-Part I: skin. *Regul. Toxicol. Pharmacol.* **2021**, *123*, 104922.
(50) Luthfianti, H. R.; Waresindo, W. X.; Edikresnha, D.; Chahyadi, A.; Suciati, T.; Noor, F. A.; Khairurrijal, K. Physicochemical characteristics and antibacterial activities of freeze-thawed polyvinyl alcohol/andrographolide hydrogels. *ACS Omega* **2023**, *8* (3), 2915−2930.
(51) Arifullah, M.; Namsa, N. D.; Mandal, M.; Chiruvella, K. K.; Vikrama, P.; Gopal, G. R. Evaluation of anti-bacterial and anti-oxidant potential of andrographolide and echiodinin isolated from callus culture of *Andrographis paniculata Nees*. *Asian Pac. J. Trop. Biomed.* **2013**, *3* (8), 604−610.
(52) Selvaraj, K.; Gayatri Devi, R.; Selvaraj, J.; Jothi Priya, A. In vitro anti-inflammatory and wound healing properties of Andrographis echioides and Andrographis paniculata. *Bioinformation* **2022**, *18*, 331−336.
(53) Burgos, R. A.; Alarcón, P.; Quiroga, J.; Manosalva, C.; Hancke, J. Andrographolide, an anti-inflammatory multitarget drug: all roads lead to cellular metabolism. *Molecules* **2021**, *26*, 5.
(54) Cai, Q.; Zhang, W.; Sun, Y.; Xu, L.; Wang, M.; Wang, X.; Wang, S.; Ni, Z. Study on the mechanism of andrographolide activation. *Front. Neurosci.* **2022**, *16*, 977376.
(55) Han, J.; Tan, C.; Pan, Y.; Qu, C.; Wang, Z.; Wang, S.; Wang, C.; Xu, K. Andrographolide inhibits the proliferation and migration of vascular smooth muscle cells via PI3K/AKT signaling pathway and amino acid metabolism to prevent intimal hyperplasia. *Eur. J. Pharmacol.* **2023**, *959*, 176082.
(56) Seo, J. Y.; Pyo, E.; An, J. P.; Kim, J.; Sung, S. H.; Oh, W. K. Andrographolide Activates Keap1/Nrf2/ARE/HO-1 Pathway in HT22 Cells and Suppresses Microglial Activation by $A\beta_{42}$through Nrf2-Related Inflammatory Response. *Mediators Inflammation* **2017**, *2017*, 1−12.
(57) Saenchoopa, A.; Plaeyao, K.; Talodthaisong, C.; Thet Tun, W. S.; Nasomjai, P.; Lapmanee, S.; Somsakeesit, L. O.; Hutchison, J. A.; Kulchat, S. Development of antibacterial hydrogels based on biopolymer aloe vera/gelatin/sodium alginate composited With SM-AgNPs loaded curcumin-nanoliposomes. *Macromol. Biosci.* **2025**, No. e2400504.
(58) Pormohammad, A.; Monych, N. K.; Ghosh, S.; Turner, D. L.; Turner, R. J. Nanomaterials in wound healing and infection control. *Antibiotics* **2021**, *10* (5), 473.
(59) Pangli, H.; Vatanpour, S.; Hortamani, S.; Jalili, R.; Ghahary, A. Incorporation of silver nanoparticles in hydrogel matrices for controlling wound infection. *J. Burn Care Res.* **2021**, *42* (4), 785−793.
(60) Lu, C. C.; Yang, J. S.; Chiu, Y. J.; Tsai, F. J.; Hsu, Y. M.; Yin, M. C.; Juan, Y. N.; Ho, T. J.; Chen, H. P. Dracorhodin perchlorate enhances wound healing via β-catenin, ERK/p38, and AKT signaling in human HaCaT keratinocytes. *Exp. Ther. Med.* **2021**, *22*, 822.
(61) Piipponen, M.; Li, D.; Landén, N. X. The immune functions of keratinocytes in skin wound healing. *Int. J. Mol. Sci.* **2020**, *21*, 8790.
(62) National Cancer Institute's Nanotechnology Characterization Laboratory Assay Cascade Protocols [Internet]. Bethesda (MD): National Cancer Institute (US); 2005 May 1-. Guide to NCL In Vivo Studies: Efficacy, Pharmacokinetics & Toxicology. 2022 Sep. Available from: https://www.ncbi.nlm.nih.gov/books/NBK604930/doi:10.17917/W63A-GR02.
(63) Siridechakorn, I.; Bhattarakosol, P.; Sasivimolrattana, T.; Anoma, S.; Wongwad, E.; Nuengchamnong, N.; Kowitdamrong, E.; Boonyasuppayakorn, S.; Waranuch, N. Inhibitory efficiency of Andrographis paniculata extract on viral multiplication and nitric oxide production. *Sci. Rep.* **2023**, *13* (1), 19738.
(64) Li, Y.; He, S.; Tang, J.; Ding, N.; Chu, X.; Cheng, L.; Ding, X.; Liang, T.; Feng, S.; Rahman, S. U.; Wang, X.; Wu, J. Andrographolide inhibits inflammatory cytokines secretion in LPS-stimulated RAW264.7 cells through suppression of NF-κB/MAPK signaling pathway. *Evidence-Based Complementary Altern. Med.* **2017**, *2017*, 8248142.
(65) More, P. R.; Pandit, S.; Filippis, A.; Franci, G.; Mijakovic, I.; Galdiero, M. Silver nanoparticles: bactericidal and mechanistic approach against drug resistant pathogens. *Microorganisms* **2023**, *11*, 369.
(66) Chang, A.; Ye, Z.; Ye, Z.; Deng, J.; Lin, J.; Wu, C.; Zhu, H. Citric acid crosslinked sphingan WL gum hydrogel films supported ciprofloxacin for potential wound dressing application. *Carbohydr. Polym.* **2022**, *291*, 119520.
(67) Fernández-Guarino, M.; Hernández-Bule, M. L.; Bacci, S. Cellular and molecular processes in wound healing. *Biomedicines* **2023**, *11* (9), 2526.
(68) Demidova-Rice, T. N.; Hamblin, M. R.; Herman, I. M. Acute and impaired wound healing: pathophysiology and current methods for drug delivery, part 2: role of growth factors in normal and pathological wound healing: therapeutic potential and methods of delivery. *Adv. Skin Wound Care* **2012**, *25* (8), 349−370.
(69) Frangogiannis, N. Transforming growth factor-β in tissue fibrosis. *J. Exp. Med.* **2020**, *217* (3), No. e20190103.
(70) João De Masi, E. C.; Campos, A. C.; João De Masi, F. D.; Ratti, M. A.; Ike, I. S.; João De Masi, R. D. The influence of growth factors on skin wound healing in rats. *Braz. J. Otorhinolaryngol.* **2016**, *82* (5), 512−521.
(71) Gimeno-Lluch, I.; Benito-Jardón, M.; Guerrero-Barberà, G.; Burday, N.; Costell, M. The role of the fibronectin synergy site for skin wound healing. *Cells* **2022**, *11* (13), 2100.
(72) Wilgus, T. A.; Ferreira, A. M.; Oberyszyn, T. M.; Bergdall, V. K.; Dipietro, L. A. Regulation of scar formation by vascular endothelial growth factor. *Lab. Invest.* **2008**, *88* (6), 579−590.
(73) Petit, I.; Levy, A.; Estrach, S.; Féral, C. C.; Trentin, A. G.; Dingli, F.; Loew, D.; Qu, J.; Zhou, H.; Théry, C.; Prunier, C.; Aberdam, D.; Ferrigno, O. Fibroblast growth factor-2 bound to specific dermal fibroblast-derived extracellular vesicles is protected from degradation. *Sci. Rep.* **2022**, *12*, 22131.
(74) Gao, M.; Guo, H.; Dong, X.; Wang, Z.; Yang, Z.; Shang, Q.; Wang, Q. Regulation of inflammation during wound healing: the function of mesenchymal stem cells and strategies for therapeutic enhancement. *Front. Pharmacol.* **2024**, *15*, 1345779.

(75) Park, J. W.; Hwang, S. R.; Yoon, I. S. Advanced growth factor delivery systems in wound management and skin regeneration. *Molecules* **2017**, *22* (8), 1259.
(76) Martin, S. F. The role of the innate immune system in allergic contact dermatitis. *Allergol. Select* **2017**, *1* (1), 39−43.
(77) Tramontana, M.; Hansel, K.; Bianchi, L.; Sensini, C.; Malatesta, N.; Stingeni, L. Advancing the understanding of allergic contact dermatitis: from pathophysiology to novel therapeutic approaches. *Front. Med.* **2023**, *10*, 1184289.
(78) So-In, C.; Sunthamala, N. Treatment efficacy of *Thunbergia laurifolia, Curcuma longa, Garcinia mangostana*, and *Andrographis paniculata* extracts in *staphylococcus aureus*-induced rabbit dermatitis model. *Vet. World* **2022**, *15*, 188−197.

https://doi.org/10.1021/acsomega.4c10648
ACS Omega 2025, 10, 10530−10545